The Thermodynamic Properties of 4,5,9,10-Tetrahydropyrene and 1,2,3,6,7,8-Hexahydropyrene

Topical Report

By
R.D. Chirico
S.E. Knipmeyer
A. Nguyen
N.K. Smith
W.V. Steele

December 1992

Work Performed Under Cooperative Agreement No. FC22-83FE60149

Prepared for
U.S. Department of Energy
Assistant Secretary for Fossil Energy

W.D. Peters, Project Manager
Bartlesville Project Office
P.O. Box 1398
Bartlesville, OK 74005

Prepared by
IIT Research Institute
National Institute for Petroleum and Energy Research
P.O. Box 2128
Bartlesville, OK 74005

MASTER

EXECUTIVE SUMMARY

Hydrogen management will be a critical issue for refiners as a result of the 1990 Amendments to the U.S. Clean Air Act. The problem stems from a reduction in hydrogen production and an increase in consumption. The addition of oxygenates to gasoline, as mandated for certain geographic areas at certain times of the year, will mean that less octane is required from the reformer, lowering the severity of the operation, and hence, the amount of hydrogen formed. Also the mandate reducing aromatics content to 25 per cent (20 per cent by proposed California state regu'ations) will result in a further reduction of reformer operating severity, hence, severely reducing hydrogen production. Another contribution to the problem in managing hydrogen results from increased hydrogen consumption to meet benzene specifications, reduced T90, and lower sulfur levels in diesel. To exacerbate the problem, as heavier crudes are introduced to the refinery, the importance of catalytic hydroprocessing will increase. Hydroprocessing can be a hydrogen guzzler.

In August 1990 the U.S. Environmental Protection Agency (EPA) announced that it is taking steps to cut the sulfur content of diesel fuel by 80 per cent -- from 0.25 weight per cent to 0.05 weight per cent -- effective October 1, 1993. In addition, the level of aromatics in diesel fuel has been the topic of several regulatory efforts in California and by the federal government. However, there exists some question of whether the proposed maximum aromatics content can be achieved and whether the aromatics content decreases concomitantly with decreases in sulfur content due to increased severity of processing conditions. In NIPER topical report NIPER-468, this problem was used as a "simple" example of thermodynamics at work in the "real world" of the process-design engineer. By introducing the concept of "crossover temperature," the report outlined, through applied thermodynamics, how to meet the conditions necessary for efficient attainment of the low aromatics levels required with concomitant sulfur level reduction.

The goal of the research programs in thermodynamics at the National Institute for Petroleum & Energy Research (NIPER), funded by the Department of Energy (DOE) Office of Fossil Energy, Advanced Extraction and Process Technology (AEPT), is the determination of the conditions under which heavier feedstocks can be processed to produce the wide slate of fuels required by modern society at prices which maintain the economic competitiveness of the U.S.A., but not conflicting with environmental regulations. The results from the thermodynamic property measurements made in these research programs are made available to the petroleum industry via NIPER Topical Reports and the peer-reviewed scientific literature.

The research is published in two types of reports. Type One, of which this is an example, details the thermochemical and thermophysical property measurements made on the representative polycyclic aromatic and hydroaromatic compounds. Type Two Reports apply the experimental information detailed in Type One Reports to thermodynamic analyses of key reaction networks involving the aromatics [e.g., derivation of the optimum conditions for formation of hydroaromatics (naphthenes), or design of hydroaromatic solvents which efficiently shuttle hydrogen to sites where the "nascent" hydrogen can be used to break asphaltenes down into smaller molecules, etc.]. Thermodynamic analyses, based on accurate information, can be used to set the boundaries (e.g., temperature range, pressure range, etc.) for efficient processing of materials, and to provide insights for the design of cost-effective methods for aromatic removal, or hydrogen shuttling.

The results reported here derive from the portion of the program providing accurate experimental thermochemical and thermophysical properties for "key" polycyclic aromatic and hydroaromatic compounds present in heavier feedstocks. This report details the thermochemical and thermophysical properties, measured at NIPER, for two hydropyrenes (4,5,9,10-tetrahydropyrene and 1,2,3,6,7,8-hexahydropyrene). Pyrene and hydropyrenes are major constituents of the heavier ends of feedstocks with low API gravity. However, no thermodynamic property measurements on hydropyrenes exist in the literature.

The property measurements reported here can be used by the process-design engineer to simulate -- on paper, without costly pilot plant experimentation -- the effects of changes in conditions on the operation of the process plant. Because the data has known uncertainty intervals, the process-design engineer can use it with the confidence that the results of the simulation would be reproduced in the pilot plant.

A companion report NIPER-601, is an example of the use of the data reported here i.e., a Type Two Report. In NIPER-601 the thermodynamic property measurements reported here are used in conjunction with previously measured values to derive an overall picture of the thermodynamics of hydrogen shuttling. The results reported in the companion report give new insights into hydrogen shuttling and the comparative effectiveness of various solvents for asphaltene dissolution.

ABSTRACT

Measurements leading to the calculation of the ideal-gas thermodynamic properties are reported for 4,5,9,10-tetrahydropyrene and 1,2,3,6,7,8-hexahydropyrene. Experimental methods included combustion calorimetry, adiabatic heat-capacity calorimetry, vibrating-tube densitometry, comparative ebulliometry, inclined-piston gauge manometry, and differential-scanning calorimetry (d.s.c.). Critical properties were estimated for both materials based on the measurement results. Entropies, enthalpies, and Gibbs energies of formation were derived for the ideal gases for selected temperatures between 380 K and 700 K. The property-measurement results reported here for 4,5,9,10-tetrahydropyrene and 1,2,3,6,7,8-hexahydropyrene are the first for these important intermediates in the pyrene/H_2 hydrogenation reaction network.

ACKNOWLEDGMENTS

TABLE OF CONTENTS

LIST OF TABLES

LIST OF FIGURES

GLOSSARY

This report is written with close adherence to the style adopted by The Journal of Chemical Thermodynamics. A complete description of the style can be found in the January 1992 issue of the journal. This glossary summarizes the main points with respect to the symbol usage.

Throughout this report only SI units are used in reporting thermodynamic values. All values are given in dimensionless units i.e., physical quantity = number X unit; for example $\rho/(kg \cdot m^{-3})$ rather than " ρ (kg/m^3)" or " ρ kg/m^3". Molar values, i.e., intensive functions, are denoted by the subscript "m", e.g., $C_{sat,m}$, whereas extensive functions do not have the subscript. In addition, since thermodynamic values are pressure dependent, they are reported in terms of a standard pressure $p°$, which in this report is 101.325 kPa (one atmosphere).

M = molar mass in $g \cdot mol^{-1}$

T = temperature in Kelvin

p = pressure in Pascals (Pa)

ρ = density in $kg \cdot m^{-3}$

$\Delta_c U_m^o$ = molar energy of combustion

$\Delta_c U_m^o / M$ = energy of combustion per gram

$\Delta_c H_m^o$ = molar enthalpy of combustion

$\Delta_f H_m^o$ = molar enthalpy of formation

$\Delta_l^g H_m$ = molar enthalpy of vaporization, hence the subscript l (for liquid) and superscript g (for gas)

$\Delta_l^g V_m$ = change in molar volume from the liquid to the real vapor

$C_{v,m}$ = molar heat capacity at constant volume

$C_{p,m}$ = molar heat capacity at constant pressure

$C_{sat,m}$ = molar heat capacity at saturated pressure

μ = chemical potential

n = number of moles of substance

V_x = volume of d.s.c. cell at a temperature T/K.

C_x^{II} = two-phase heat capacity at cell volume V_x

C_v^{II} = two-phase heat capacity at constant volume

$C_v^{II} (\rho = \rho_{sat})$ = two-phase heat capacity along the saturation line

V_l = molar volume of the liquid

T_c = critical temperature

p_c = critical pressure

ρ_c = critical density

T_r = reduced temperature = T/T_c

p_r = reduced pressure = p/p_c

ρ_r = reduced density = ρ/ρ_c

lg = $\log_{10}$

ω = acentric factor = $[-\text{lg}\,(p_x/p_c) - 1]$; p_x is the vapor pressure at T_r = 0.7

$\Delta_0^T S_m^o$ = molar entropy at temperature T/K (relative to the entropy at T = 0 K)

$\Delta_0^T H_m^o$ = molar enthalpy at temperature T/K (relative to the crystals at 0 K)

$\Delta_{comp} S_m$ = molar entropy of compression of a gas

$\Delta_{imp} S_m$ = gas imperfection term

T $\rightarrow$ 0 = Zero Kelvin

To avoid listing units in tables, entropies are reported as divided by the gas constant R, and enthalpies and Gibbs energies are generally reported divided by the product of the gas constant and temperature, R·T. Units of time are s (seconds), d (days), and h (hours).

1. INTRODUCTION

Within the petroleum industry, the use of catalytic hydroprocessing is increasing.[1]§ Its application continues to grow as crudes become heavier and the range of specialty products increases. Over time its use can only continue to increase with the anticipated processing of oil shale, tar sands, and eventually the products of the liquefaction of coal. Important areas within catalytic hydroprocessing include the hydrogenation of aromatics, hydrodesulfurization (HDS), hydrodenitrogenation (HDN) and hydrodeoxygenation (HDO). This report is the product of research funded by the U. S. Department of Energy's (DOE) Office of Fossil Energy, Advanced Extraction & Process Technology Program (AEPT). Within a portion of that research program, the thermochemical and thermophysical properties are determined for "key" aromatics and hydroaromatics present in the spectrum of fossil-fuel materials. The results of the thermodynamic-property measurements will be used to provide insights into the reaction networks and relative reactivities of polycyclic aromatics and hydroaromatics within the complicated processes operating in hydroprocessing.

Hydroaromatic (hydrogen donor) compounds will play an important role in the development of processes for the whole spectrum of fossil fuel materials from heavy petroleum through coal. For example, in the processing of some heavy petroleums and *all* coal liquids the naphtha fraction will contain relatively large amounts of two-ring aromatics, which have a strong tendency to form coke on catalysts during reforming. A simplistic answer to the problem would be cutting the naphtha at 300 °F rather than 375-400 °F. Since that would decrease the naphtha yield and make the process uneconomic, hydrocracking of the two-ring structures via the formation of hydro-aromatics may be a better answer to the problem. The comments of Fisher and Wilson[2] then become relevant.

"Predictive schemes are available using group additivity concepts for calculating, thermodynamic properties of complex aromatic molecules. Such schemes must rely on accurately measured thermochemical data for the calculation of reliable group additivity values. The lack of such data for the bicyclic and tricyclic species present in these distillates argues against attempting to predict their free energy values."

For the "simple" single-ring aromatics, Fisher and Wilson were able to use the available thermodynamic data to conclude, "thermodynamic limitations to saturation of

---

§   References are listed in numerical order at the end of this report.

aromatics were found to predominate at the higher temperatures, and complete conversion in synthetic distillates was only achieved well removed from thermodynamic constraints." When the thermodynamic constraints are unknown, or can only be estimated within large error bands, for the larger systems so important to the alternate crudes, how can the process-design engineer know what is "well removed" from them?

Several groups have reported in the recent literature the presence of a coal-resid synergy.[3-11] An understanding of the reason(s) for this synergy could transform coal-liquefaction technology. However, at present no such understanding exists. It may be that the non-donor species (polycyclic aromatic hydrocarbons in all examples to date) react with the donor solvent forming reactive species which engender hydrogenolysis and liquefaction of the coal.[8] If that is true, then, with the choice of a suitable system, there is the possibility of coal liquefaction at lower temperatures. Also, the hydrogen addition could be tailored to specific sites within the coal structure cutting the formation of light gases (C_1 through C_4), which wastes expensive hydrogen.

Alternatively, it may be possible that the whole synergy is caused by increased solvation effects due to the high operational temperatures.[9,10] For example, the reaction temperature (425 °C) in the research of Cassidy et al.[11] is above the critical temperature of one of the solvent components, decalin, but below the critical temperatures of either naphthalene or tetralin (two of the other major components). Therefore, the physical states of the various mixtures are difficult to specify, especially since the critical temperatures are mostly estimates with large uncertainties. The effect could be just another example of supercritical solvent extraction. In the absence of thermodynamic properties on key partially hydrogenated polycyclic aromatic hydrocarbons, the basis for the synergy will remain conjecture.

This report details the thermochemical and thermophysical properties, measured at NIPER, for two hydropyrenes (4,5,9,10-tetrahydropyrene and 1,2,3,6,7,8-hexahydropyrene). Pyrene and hydropyrenes are major constituents of the heavier ends of feedstocks with low API gravity. Pyrene and hydropyrenes are also major components of effective solvents for the dissolution of asphaltenes and the initial liquefaction of coal.[5] No thermodynamic-property measurements on these important compounds existed in the literature prior to the measurements reported here.

2. EXPERIMENTAL

MATERIALS

The sample of 4,5,9,10-tetrahydropyrene was synthesized as follows. Pyrene (220 g) was desulfurized by treating with Raney-nickel catalyst in alkaline (ethanol+water)

solution, and was hydrogenated for a period of 24 h at 0.3 MPa pressure and 333 K in the presence of 5 per cent Pd/C catalyst in 1.5 dm³ of acetic acid. G.l.c. analysis showed the product was 61 per cent 4,5,9,10-tetrahydropyrene. Recrystallization from 2-methylpentane and passage through a picric acid column gave 110 g of product of mole fraction 0.95. Additional purification was attained by catalytic hydrogenation for a period of 24 h at 0.4 MPa pressure and 333 K in the presence of 8 g Pd/C catalyst in ethyl acetate. This treatment improved the purity to mole fraction 0.99. Further treatment consisted of Soxhlet extraction through a bed of neutral and basic alumina with hexane, under argon, and allowing the sample to crystallize near 295 K. The purified crystals were dried under vacuum at 350 K.

1,2,3,6,7,8-Hexahydropyrene was synthesized as follows. Pyrene (200 g) was reduced with sodium (180 g) in 4.5 dm³ of pentan-1-ol at reflux temperature. G.l.c. analysis showed the product was 58 per cent 1,2,3,6,7,8-hexahydropyrene. Recrystallization from hexane yielded a product of 0.99 mole fraction purity. This material was Soxhlet extracted through a bed of neutral and basic alumina with hexane, under argon. The resulting solid was recrystallized from {5 n-hexane (C_6H_{14}) + 1 diethylether $(C_4H_{10}O)$} and dried under vacuum at 350 K.

Mole-fraction impurities for each sample were determined by fractional melting as part of the adiabatic heat-capacity calorimetric studies. The mole-fraction impurities were 0.00016 and 0.00018 for 4,5,9,10-tetrahydropyrene and 1,2,3,6,7,8-hexahydropyrene, respectively. The high purities of the samples were corroborated by the small differences between the boiling and condensation temperatures observed in the ebulliometric vapor-pressure studies.

The water used as a reference material in the ebulliometric vapor-pressure and density measurements was deionized and distilled from potassium permanganate. The decane used as a reference material for the ebulliometric measurements was purified by urea complexation, two recrystallizations of the complex, its decomposition with water, extraction with ether, drying with $MgSO_4$, and distillation at 337 K and 1 kPa pressure.

PHYSICAL CONSTANTS AND STANDARDS

Molar values are reported in terms of M = 206.287 g·mol⁻¹ and 208.303 g·mol⁻¹ for 4,5,9,10-tetrahydropyrene and 1,2,3,6,7,8-hexahydropyrene, respectively, based on the relative atomic masses of 1981[12]† and the gas constant

---

† The 1981 relative atomic masses were used because the CODATA Recommended Key Values for Thermodynamics (reference 39) are based on them.

3

$R = 8.31451$ J·K^{-1}·mol^{-1} adopted by CODATA.[13] The platinum resistance thermometers used in these measurements were calibrated by comparison with standard thermometers whose constants were determined at the National Institute of Standards and Technology (NIST), formerly the National Bureau of Standards (NBS). All temperatures reported are in terms of the IPTS-68.[14] The platinum resistance thermometer used in the adiabatic heat-capacity studies was calibrated below 13.81 K with the method of McCrackin and Chang.[15] Measurements of mass, time, electrical resistance, and potential difference were made in terms of standards traceable to calibrations at NIST.

APPARATUS AND PROCEDURES

Densitometry. Densities reported previously by this research group were obtained in a densitometer,[16] which had an upper temperature limit of approximately 430 K. Studies on high-molecular-weight compounds (three aromatic rings and greater) required that this upper temperature limit be raised substantially. As a result the densitometer described here has an upper temperature limit near 520 K (the limit at present is set by that attainable by the constant temperature bath.) The design of the new densitometer is essentially that used successfully by Dr. J. M. Simonson and his colleagues at Oak Ridge National Laboratory¥ for the study of aqueous salt mixtures at high temperatures and pressures.

Figure 1 is a schematic figure of the densitometry apparatus. The stainless-steel vessel **I** contained the liquid sample whose density was to be determined. A six-port gas-chromatography (g.c.) valve (ports number 1 through 6 in figure 1) was used to isolate helium, water or vacuum from the sample and the sample cell. The vibrating tube **P**, made at NIPER to a design obtained from Dr. Simonson, had a volume of about 2 cm^3. The vacuum traps **A** and **Q** were used in evacuating sample or water from the vibrating tube. The three-way valves **K** and **N** were used to control the flow of helium and water respectively, into and out of the vibrating tube. Water pressure was read from the pressure gauge **M**. All elements shown within perimeter **R** were thermostatted to ±0.005 K in an air bath. A 25-Ω platinum resistance thermometer (Leeds and Northrup) was positioned in a well close to the six-port g.c. valve. A differential (iron-to-constantan) thermocouple with one junction attached to the platinum resistance thermometer well and the other to the densitometer cell, was used to monitor

Figure 1.   Schematic of densitcmeter.   I, sample cell; P, vibrating tube densitometer; A and Q, vacuum traps; C, E, K, and N, three-way valves; B, D, F, G, H, J, L, and O, two-way valves; M, pressure gauge for water pressure measurement; R, boundary of thermostatted region.

temperature gradients. An Anton-Paar DMA 512 and DMA 60 were used to drive the vibrating tube and measure the frequency of vibration, respectively.

For measurement of density approximately 6 cm^3 of sample was transferred into the evacuated sample cell **I**, which was connected to the apparatus as shown in figure 1. The entire system up to valve **G** was evacuated to approximately 1 x 10^{-5} Pa and then isolated from the vacuum pumps (oil diffusion pump and rotary roughing pump). With valve **H** closed, the six-port g.c valve was switched to connect the vibrating tube **P** to the sample cell, as shown in figure 1. Valve **G** was opened to let sample into the vibrating tube. The air bath was heated to the required temperature, and when thermal equilibrium was reached (as denoted by the differential thermocouple, and stabilization of the vibration frequency) the vibration frequency was recorded. Vibrational frequencies at successively high temperatures were obtained without removal of the sample from the vibrating tube. After the measurement at the highest temperature, valves **B** and **O** were closed. On opening valve **J**, helium at a pressure slightly above the vapor pressure of the sample was let into the system up to valve **H**. The helium was used to push the sample back into cell **I**. Then valves **G** and **J** were shut off and valve **B** was opened to pump the remaining sample out of the vibrating tube through vacuum trap **Q**. Then the six-port g.c. valve was switched for system calibration (as shown by dashed lines in figure 1). Valves **O** and **D** were opened to evacuate both sides of the densitometer cell and the vibrating tube evacuated to approximately 1 x 10^{-5} Pa. Vibrational frequencies for the evacuated vibrating tube were determined for each of the temperatures at which values for the liquid were previously measured.

For calibration of the densitometer with water as the standard, valves **B**, **D**, **F** and **O** were closed and the three-way valves **E** and **N** opened to the direction of exhaust and water, respectively. Valve **L** was opened and the water pump turned on. The system was pressurized to 60 bar and the water pressure slowly reduced by carefully opening valve **F**. The pressure was lowered to a value approximately one bar above the vapor pressure of water at the temperature of the air bath.[17] Vibrational frequencies for the water-filled vibrating tube were determined for each of the temperatures at which values for the compound under study were measured previously.

For each temperature a calibration constant for the densitometer was derived with the equation:

$$(\rho_w - \rho_v) / \rho^0 = K(\tau_w^2 - \tau_v^2) / (\tau^0)^2 ,$$

(1)

6

where ρ^0 and τ^0 are 1.0 kg·m^{-3} and 1.0 s, respectively. ρ_w is the density of water in kg·m^{-3} as per reference 17. The density of the vacuum ρ_v was assumed to be zero. τ_w and τ_v are the vibration periods in seconds for water and a vacuum in the densitometer, respectively. Densities for the hydropyrenes were derived with the equation:

$$(\rho_1 - \rho_2) / \rho^\circ = K(\tau_1^2 - \tau_2^2) / (\tau^0)^2 , \qquad (2)$$

were τ_i is the resonance period of the tube when filled with a fluid of density ρ_i.

Measurements of the density of benzene were made between 310 K and 523 K to determine the accuracy of the results obtained with the densitometer. Results agreed with the values published by Hales and Townsend[18] within ±0.1 per cent. The precision of the measurements was approximately 0.05 per cent.

Combustion Calorimetry. The experimental procedures used in the combustion calorimetry of organic compounds at the National Institute for Petroleum and Energy Research have been described.[19-21] A rotating-bomb calorimeter (laboratory designation BMR II)[22] and platinum-lined bomb (laboratory designation Pt-3b)[23] with an internal volume of 0.3934 dm^3 were used without rotation. For each experiment, 1.0 x 10^{-3} dm^3 of water was added to the bomb, and the bomb was flushed and charged to 3.04 MPa with pure oxygen. Judicious choice of sample and auxiliary masses allowed the temperature rise in each combustion series and its corresponding calibration series to be the same within 0.1 per cent. All experiments were completed within 0.01 K of 298.15 K.

Temperatures were measured by quartz-crystal thermometry.[24,25] A computer was used to control the combustion experiments and record the results. The quartz-crystal thermometer was calibrated by comparison with a platinum resistance thermometer. Counts of the crystal oscillation were taken over periods of 100 s throughout the experiments. Integration of the time-temperature curve is inherent in the quartz-crystal thermometer readings.[26]

Ebulliometric Vapor-Pressure Measurements. The essential features of the ebulliometric equipment and procedures are described in the literature.[27,28] The ebulliometers were used to reflux the substance under study with a standard of known vapor pressure under a common helium atmosphere. The boiling and condensation temperatures of the two substances were determined, and the vapor pressure was derived with the condensation temperature of the standard.[29]

The precision in the temperature measurements for the ebulliometric vapor-pressure studies was 0.001 K. The precision in pressure is adequately described by:

$$\sigma(p) = (0.001 \ K)\{(dp_{ref}/dT)^2 + (dp_x/dT)^2\}^{1/2} , \qquad (3)$$

where p_{ref} is the vapor pressure of the reference substance and p_x is the vapor pressure of the sample under study. Values of dp_{ref}/dT for the reference substances were calculated from fits of the Antoine equation[30] to vapor pressures of the reference materials (decane and water) reported in reference 29.

Inclined-Piston Vapor-Pressure Measurements. The equipment for the inclined-piston vapor-pressure measurements has been described by Douslin and McCullough,[31] and Douslin and Osborn.[32] Recent revisions to the equipment and procedures have been reported.[16] Uncertainties in the pressures determined with the inclined-piston apparatus, on the basis of estimated precision of measuring the mass, area, and angle of inclination of the piston, are adequately described by the expression:

$$\sigma(p) = 1.5 \times 10^{-4} p + 0.2 \ Pa. \qquad (4)$$

The uncertainties in the temperatures are 0.001 K.

Adiabatic Heat-Capacity Calorimetry. Adiabatic heat-capacity and enthalpy measurements were made with a calorimetric system described previously.[16] The calorimeter characteristics and sealing conditions are given in table 1.[1] Energy measurement procedures were the same as those described for studies on quinoline.[16] Thermometer resistances were measured with self-balancing, alternating-current resistance bridges (H. Tinsley & Co. Ltd.; Models 5840C and 5840D). Energies were measured to a precision of 0.01 per cent, and temperatures were measured to a precision of 0.0001 K. The energy increments to the filled platinum calorimeter were corrected for enthalpy changes in the empty calorimeter, for the helium exchange gas, and for vaporization of the sample. The maximum correction to the measured energy for the helium exchange gas was 0.1 per cent near 5 K. The sizes of the other two corrections are indicated in table 1.

Differential-Scanning Calorimetry (d.s.c.). Differential-scanning calorimetric measurements were made with a Perkin-Elmer DSC-2. Experimental methods were described previously.[33-35]

---

1 All tables are given at the end of this report.

3. RESULTS

DENSITY MEASUREMENTS

Measured densities for 4,5,9,10-tetrahydropyrene and 1,2,3,6,7,8-hexahydropyrene in the liquid phase (temperature range 423 K to 523 K) are listed in table 2.

COMBUSTION CALORIMETRY

NIST thermochemical benzoic acid (sample 39i) was used for calibration of the combustion calorimeter; its specific energy of combustion is $-(26434.0 \pm 3.0)$ $J \cdot g^{-1}$ under certificate conditions. Conversion to standard states[36] gives $-(26413.7 \pm 3.0)$ $J \cdot g^{-1}$ for $\Delta_c U_m^o / M$, the specific energy of the idealized combustion reaction. Calibration experiments were interspersed with the hydropyrene measurements. Nitrogen oxides were not formed in the experiments due to the high purity of the oxygen used and preliminary bomb flushing. The energy equivalent of the calorimeter obtained for the calibration series, ε(calor), was (16771.5 ± 0.6) $J \cdot K^{-1}$ (mean and standard deviation of the mean). For the cotton fuse, empirical formula $CH_{1.774}O_{0.887}$, $\Delta_c U_m^o / M$ was -16945 $J \cdot g^{-1}$.

Auxiliary information, necessary for reducing apparent mass to mass, converting the energy of the actual bomb process to that of the isothermal process, and reducing to standard states,[36] included densities at 298.15 K of 1338 $kg \cdot m^{-3}$ and 1178 $kg \cdot m^{-3}$ for crystalline 4,5,9,10-tetrahydropyrene and 1,2,3,6,7,8-hexahydropyrene, respectively. For both compounds, an estimated value of 5×10^{-7} $m^3 \cdot K^{-1}$ for $(\partial V_m / \partial T)_p$ was used in the reduction to standard states. The compounds were burned in the form of pellets. The densities were obtained by weighing pellets of known volume. The molar heat capacity at 298.15 K for each hydropyrene used in the corrections to standard states is given later as part of the heat-capacity study results.

Carbon dioxide was recovered from the combustion products of each experiment. Anhydrous lithium hydroxide was used as absorbent.[37] The combustion products were checked for unburned carbon and other products of incomplete combustion, but none was detected. Carbon dioxide recoveries were 99.983 ± 0.024 per cent (mean and standard deviation of the mean) for the calibrations, 99.987 ± 0.018 per cent for the 4,5,9,10-tetrahydropyrene combustions, and 99.986 ± 0.010 per cent for the 1,2,3,6,7,8-hexahydropyrene combustions.

Typical combustion experiments for 4,5,9,10-tetrahydropyrene and 1,2,3,6,7,8-hexahydropyrene are summarized in table 3. It is impractical to list

9

summaries for each combustion, but values of $\Delta_c U^o_m/M$ for all the experiments are reported in table 4. All values of $\Delta_c U^o_m/M$ in table 4 refer to the reaction:

$$C_aH_b(cr) + (a + b/4)O_2(g) = a\ CO_2(g) + (b/2)H_2O(l). \tag{5}$$
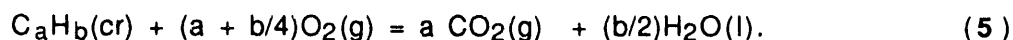
Table 4 also gives derived values of the standard molar energy of combustion $\Delta_c U^o_m$, the standard molar enthalpy of combustion $\Delta_c H^o_m$, and the standard molar enthalpy of formation $\Delta_f H^o_m$ for 4,5,9,10-tetrahydropyrene and 1,2,3,6,7,8-hexahydropyrene. Values of $\Delta_c U^o_m$ and $\Delta_c H^o_m$ refer to reaction (5). The values of $\Delta_f H^o_m$ refer to reaction (6):

$$a\ C(cr,\ graphite) + (b/2)H_2(g) = C_aH_b(cr). \tag{6}$$
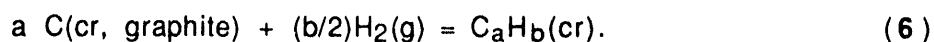
Uncertainties given in table 4 are the "uncertainty interval" defined in reference 38. The enthalpies of formation of $CO_2(g)$ and $H_2O(l)$ were taken to be -(393.51±0.13) kJ·mol^{-1} and -(285.830 ± 0.042) kJ·mol^{-1}, respectively, as assigned by CODATA.[39]

VAPOR-PRESSURE MEASUREMENTS

Vapor pressures for 4,5,9,10-tetrahydropyrene and 1,2,3,6,7,8-hexahydropyrene are reported in table 5. Following previous practice,[28] the results obtained in the ebulliometric measurements were adjusted to common pressures. The common pressures, the condensation temperatures, and the difference between condensation and boiling temperatures ΔT for the samples are reported. For both samples the small differences between the boiling and condensation temperatures (column 6 table 5) indicated correct operation of the equipment and the high purity of the samples. At the highest temperatures measured for each sample, the larger values of ΔT relative to the previous temperatures are indicative of sample decomposition.

ADIABATIC HEAT-CAPACITY CALORIMETRY

Crystallization and Melting Studies. Crystallizations of 4,5,9,10-tetrahydropyrene and 1,2,3,6,7,8-hexahydropyrene were initiated by slowly cooling (approximately 4.5 mK·s^{-1}) the liquid samples. Nucleation occurred approximately 3 K below the triple-point temperature for 4,5,9,10-tetrahydropyrene and 10 K below the triple-point temperature for 1,2,3,6,7,8-hexahydropyrene. Complete crystallization was ensured by maintaining the samples under adiabatic conditions in the partially melted state (10 per cent to 20 per cent liquid) for approximately 4 h. No spontaneous

warming, which would indicate incomplete crystallization, was observed in this time period. The samples were cooled at an effective rate of $4 \, mK \cdot s^{-1}$ to crystallize the remaining liquid. Finally, the samples were thermally cycled from approximately 280 K to within 2 K of the triple-point temperatures, where they were held for a minimum of 6 h to provide further tempering. All of the solid-phase measurements were performed upon crystals pre-treated in this manner.

The triple-point temperatures T_{tp} and sample purities were determined by measurement of the equilibrium melting temperatures $T(F)$ as a function of fraction F of the sample in the liquid state.[40] Equilibrium melting temperatures were determined by measuring temperatures at approximately 300-s intervals for 1 to 1.5 h after an energy input and extrapolating to infinite time by assuming an exponential decay toward the equilibrium value. The observed temperatures at 1 h after an energy input were invariably within 3 mK of the calculated equilibrium temperatures for F values listed in table 6. No evidence for the presence of solid-soluble impurities was found for either sample. Published procedures[40] were used to derive the apparent mole fraction of impurities and triple-point temperatures. The results are summarized in table 6.

Phase Transformations and Enthalpy Measurements. Experimental molar enthalpy results are summarized in table 7. The table includes both phase-transition enthalpies and single-phase measurements, which serve as checks on the integration of the heat-capacity results. Corrections for pre-melting caused by impurities were made in these evaluations. Results with the same series number in tables 7 and 8 were taken without interruption of adiabatic conditions.

Excellent reproducibility (within ± 0.02 per cent) was obtained in the enthalpy-of-fusion results. This implies that phase cr(I) was formed reproducibly for both compounds by means of the tempering methods described above. 4,5,9,10-Tetrahydropyrene showed three solid phases with transitions near 319.9 K and 385.1 K. 1,2,3,6,7,8-Hexahydropyrene showed two solid phases with a transition near 377.0 K. The complete heat-capacity curves are shown in figures 2 and 3.

For 4,5,9,10-tetrahydropyrene, conversion of phase cr(I) to phase cr(II) was achieved easily by cooling, and excellent reproducibility was obtained in the enthalpy-of-transition results. Details of measurements made and subsequently derived heat-capacities for the cr(II)-to-cr(I) phase-change region are shown in figure 4. The heat-capacity curve shown in this and other figures is consistent with the measurement results. The shape of the curve is not defined uniquely near T_{trs} for each
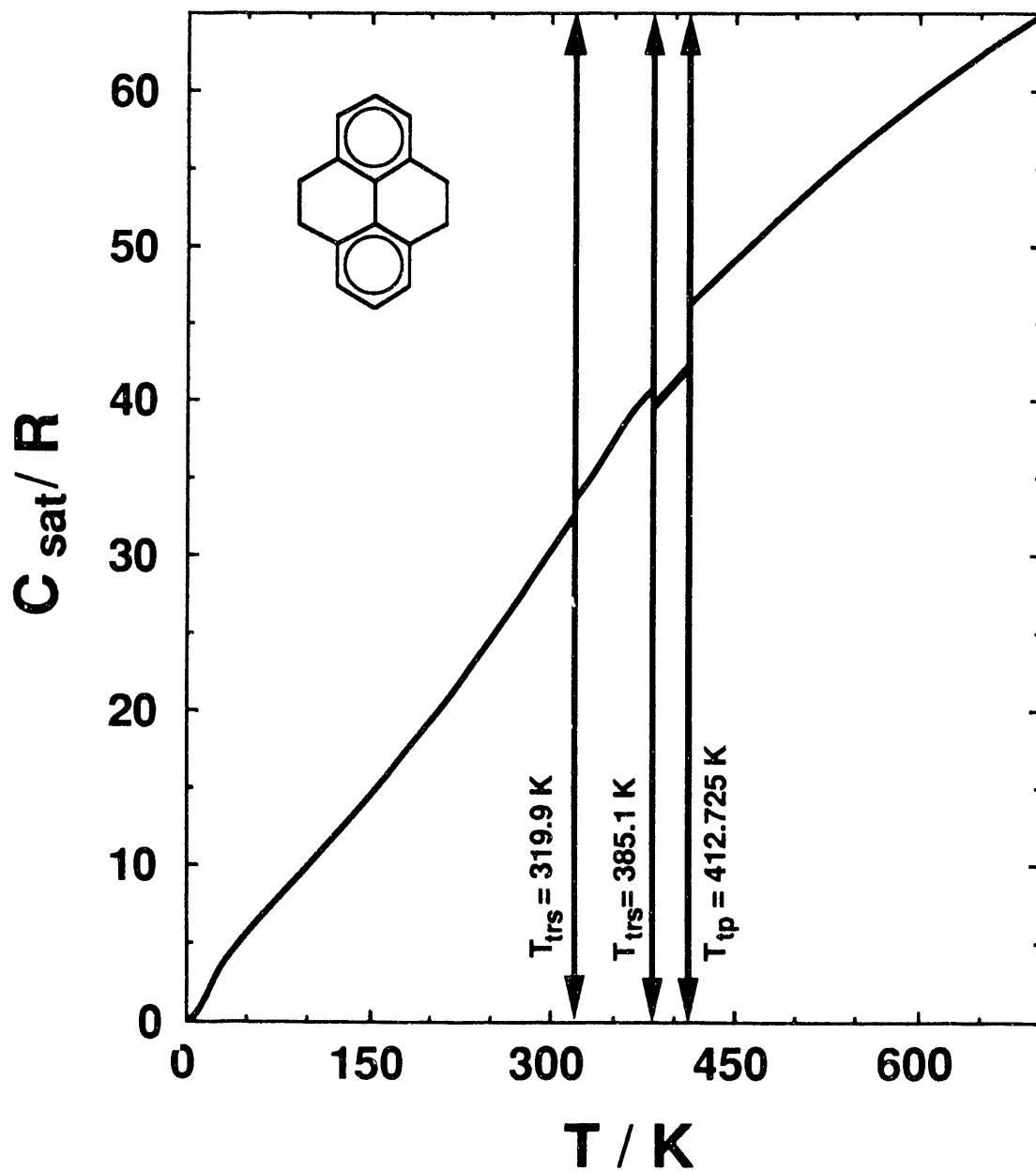
Figure 2. Curve of heat capacity against temperature for 4,5,9,10-tetrahydropyrene. The vertical lines indicate phase-transition temperatures.
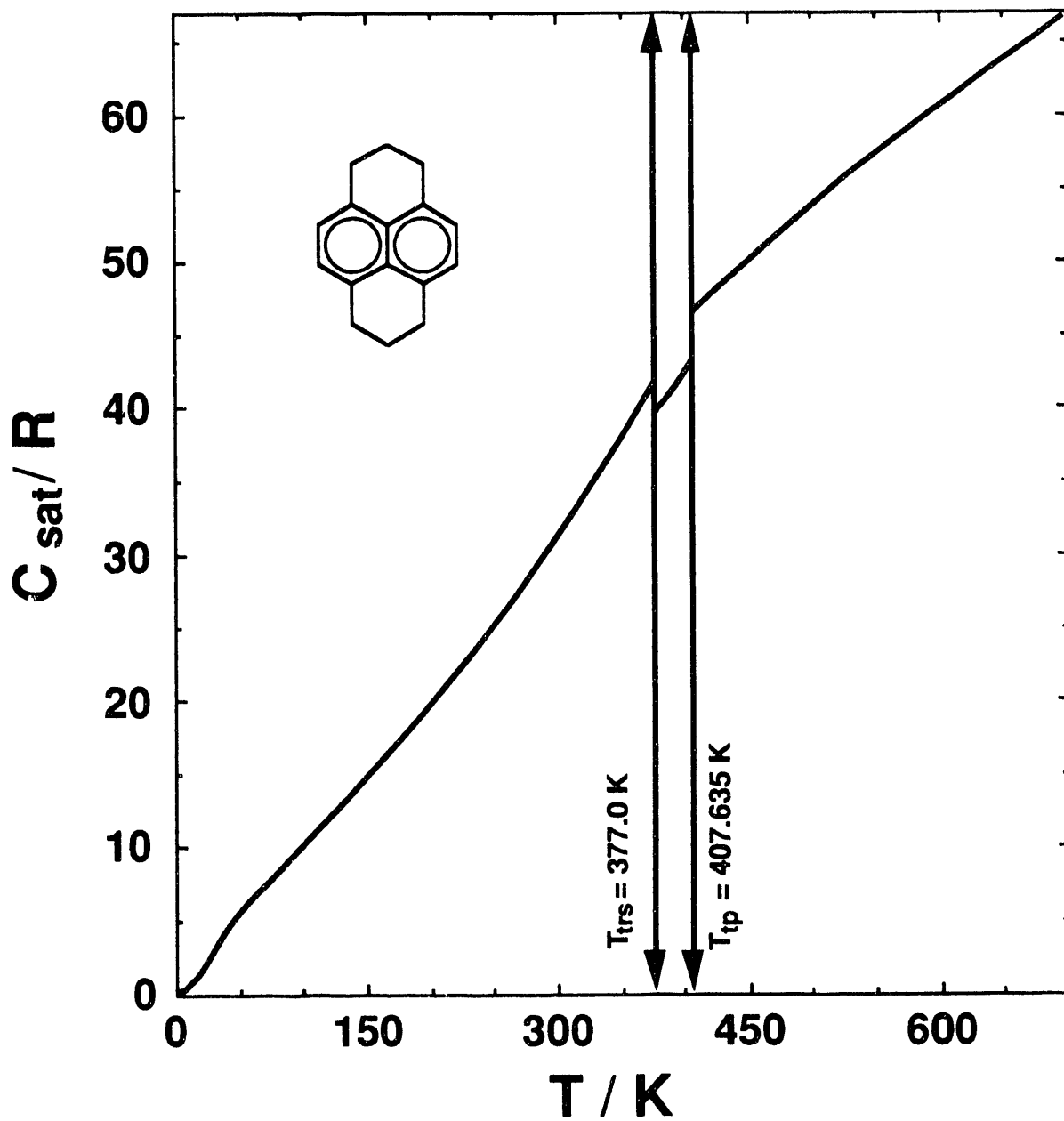
Figure 3. Curve of heat capacity against temperature for 1,2,3,6,7,8-hexahydropyrene. The vertical lines indicate phase-transition temperatures.

Figure 4. Average heat capacities in the cr(II)-to-cr(I) transition region for 4,5,9,10-tetrahydropyrene. ●, Series 2; ▲, series 3; □, series 4; ■, series 5; △, series 20. The horizontal bars span the temperature increment associated with each average heat-capacity value. The vertical line indicates the phase-transition temperature. The heat-capacity curve is not defined uniquely between 383 K and 387 K. See text.

transformation. However, this uncertainty does not have a significant effect on the uncertainty of the derived thermodynamic functions.

The transition temperature T_{trs} for the cr(II)-to-cr(I) phase change in 4,5,9,10-tetrahydropyrene was determined as part of the series-4 results. Sufficient energy was added to the sample to convert 0.87 of phase cr(II) to phase cr(I). The sample was maintained under adiabatic conditions in this partially converted state for 3 d. In this time period the sample did not reach equilibrium; however, an estimate of the temperature could be made; (385.10 ± 0.05) K. This value was taken as T_{trs} for this phase change.

Conversion of phase cr(II) to phase cr(III) in 4,5,9,10-tetrahydropyrene required approximately 20 d of annealing near 310 K. Prior to measurements of the transition enthalpy, the sample was annealed for 11 d, 20 d, and 28 d for series 10, 15, and 19, respectively. No warming was detected after approximately 12 d of annealing. This is consistent with the enthalpy-of-transition results listed in table 7. The average of the series-15 and series-19 results was used to calculate the enthalpy of transition.

Nucleation of the conversion to cr(III) did not occur unless the sample was cooled well below T_{trs}. Heat-capacity measurements for cr(II) were made to 287 K, although T_{trs} for conversion to cr(III) was found to be 319.9 K, as described below. No attempt was made to measure heat capacities for cr(II) below 287 K. When the sample was cooled below 200 K, conversion to cr(III) was usually apparent on reheating to near 300 K, as evidenced by spontaneous warming. However, on several occasions the sample was cycled between 310 K and 80 K without evidence of transformation.

An estimate of T_{trs} was obtained as part of the series-19 measurements by adding sufficient energy to convert 0.81 of the sample from phase cr(III) to phase cr(II) and allowing the sample to approach equilibrium over a period of 7.2 d. At the end of this period the 4,5,9,10-tetrahydropyrene had not equilibrated completely, but an estimate of T_{trs}, (319.9 ± 0.1) K, could be made. The uncertainty in T_{trs} has an insignificant effect on the precision of the derived thermodynamic functions. Details of measurements made in the cr(III)-to-cr(II) phase-change region are shown in figure 5.

Equilibrium was reached in less than 1 h for heat-capacity measurements in the liquid phase for 4,5,9,10-tetrahydropyrene. Equilibration times for phase cr(III) were less than 1 h for all temperatures below 315 K. Equilibration times increased rapidly above this temperature for cr(III). As noted above, equilibration times at the cr(III)-to-cr(II) transition temperature exceeded 7 d. For phase cr(II), equilibration
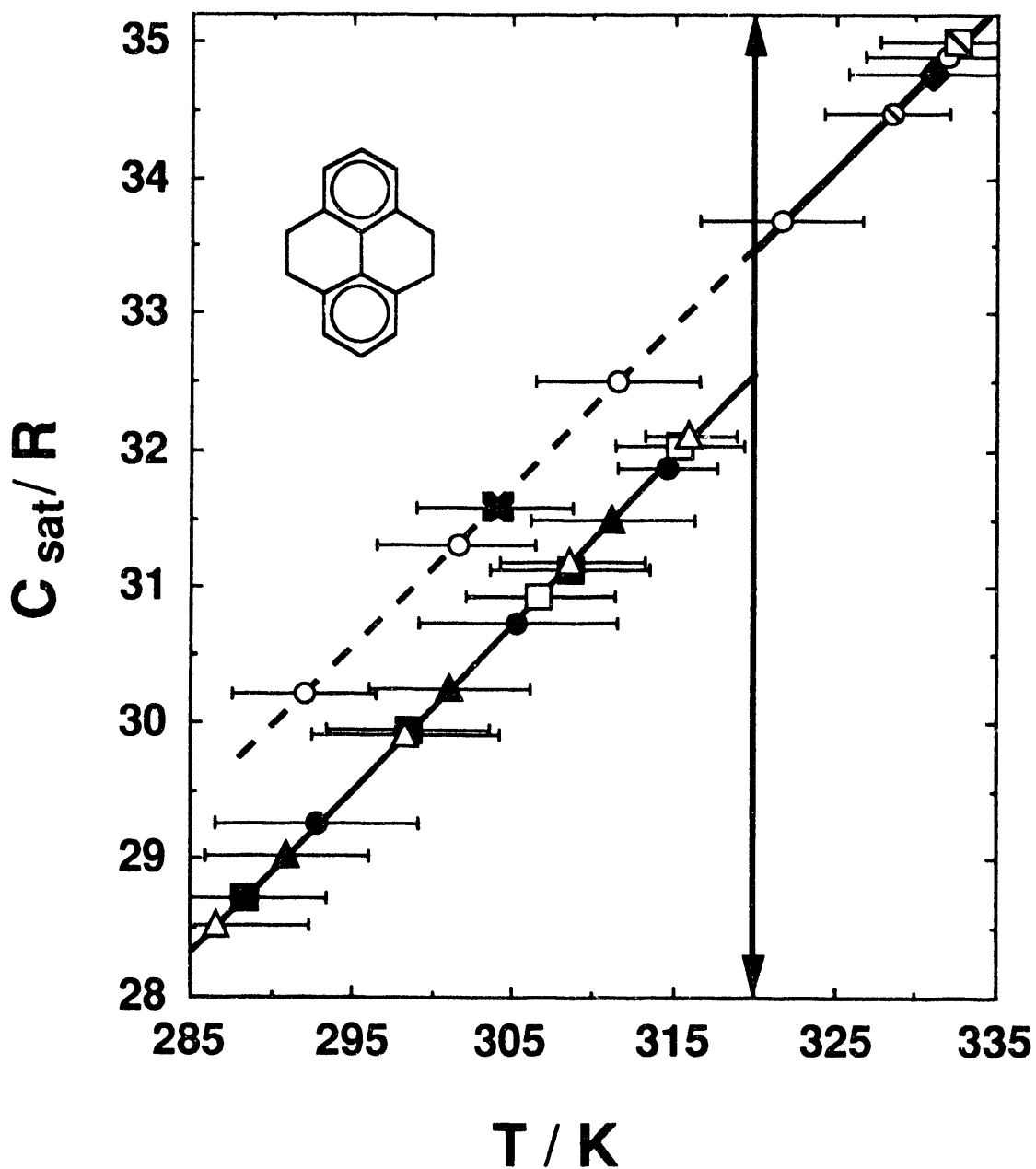
Figure 5. Average heat capacities in the cr(III)-to-cr(II) transition region for 4,5,9,10-tetrahydropyrene. ◯, Series 5; ◳, series 6; ◼, series 9; ●, series 10; ☐, series 11; △, series 12; ◆, series 16; ✖, series 17; ▲, series 18; ◐, series 19. Results of measurements spanning T_{trs} (series 2, series 4, series 5, and series 20) are not shown. These are listed in table 9. The horizontal bars span the temperature increment associated with each average heat-capacity value. The vertical line indicates the phase-transition temperature; ---, represents the heat-capacity curve for supercooled phase cr(I). See text.

16

times were less than 1 h between 285 K and 340 K, and increased to 2 h at 350 K, 6 h at 370 K, 12 h at 380, and >72 h at T_{trs}; 385.1 K. If phase cr(III) had been formed, the equilibration time on first transforming from cr(III) to cr(II) was approximately 2 d. Subsequent measurements in cr(II) showed no dependence on the thermal history. Equilibration times for phase cr(I) were approximately 8 h and were independent of temperature.

For 1,2,3,6,7,8-hexahydropyrene, conversion of phase cr(I) to phase cr(II) was achieved easily by cooling, and excellent reproducibility was obtained in the enthalpy-of-transition results. The results of series 4 and of series 12 were averaged to calculate the enthalpy-of-transition value. The results of series 3 and of series 6 were obtained over much longer time periods, and therefore, have larger uncertainties due to heat-leaks. Details of measurements made and subsequently derived heat-capacities for the cr(II)-to-cr(I) phase-change region are shown in figure 6.

The transition temperature T_{trs} for the cr(II)-to-cr(I) phase change in 1,2,3,6,7,8-hexahydropyrene was determined as part of the series-6 results. Sufficient energy was added to the sample to convert 0.44 and 0.77 of phase cr(II) to phase cr(I). The sample was maintained under adiabatic conditions in this partially converted state for 3 d at each conversion fraction. In this time period the sample did not reach equilibrium at either fraction. The equilibrium temperatures associated with the conversion fractions were estimated to be 376.98 K and 376.99 K for conversion fractions 0.44 and 0.77, respectively. The transition temperature was estimated to be (377.00 ± 0.03) K.

Equilibrium was reached in less than 1 h for heat-capacity measurements in the liquid phase for 1,2,3,6,7,8-hexahydropyrene. For phase cr(II), equilibration times were less than 1 h below 340 K, and increased to 2 h at 350 K, 7 h at 370 K, 12 h at 375, and >72 h at T_{trs}; 377.0 K. Equilibration times for phase cr(I) were approximately 4 h for all temperatures less than 400 K, and increased to 8 h at 405 K.

The experimental molar heat capacities under vapor saturation pressure $C_{sat,m}$ determined by adiabatic calorimetry are listed in table 8. Values in table 9 were corrected for effects of sample vaporization into the gas space of the calorimeter. The temperature increments were small enough to obviate the need for corrections for non-linear variation of $C_{sat,m}$ with temperature except near the solid-phase transition temperatures. The precision of the heat-capacity measurements ranged from approximately 5 per cent at 5 K, to 2 per cent at 10 K, 0.2 per cent near 20 K, and improved gradually to less than 0.1 per cent above 100 K, except in the solid phases
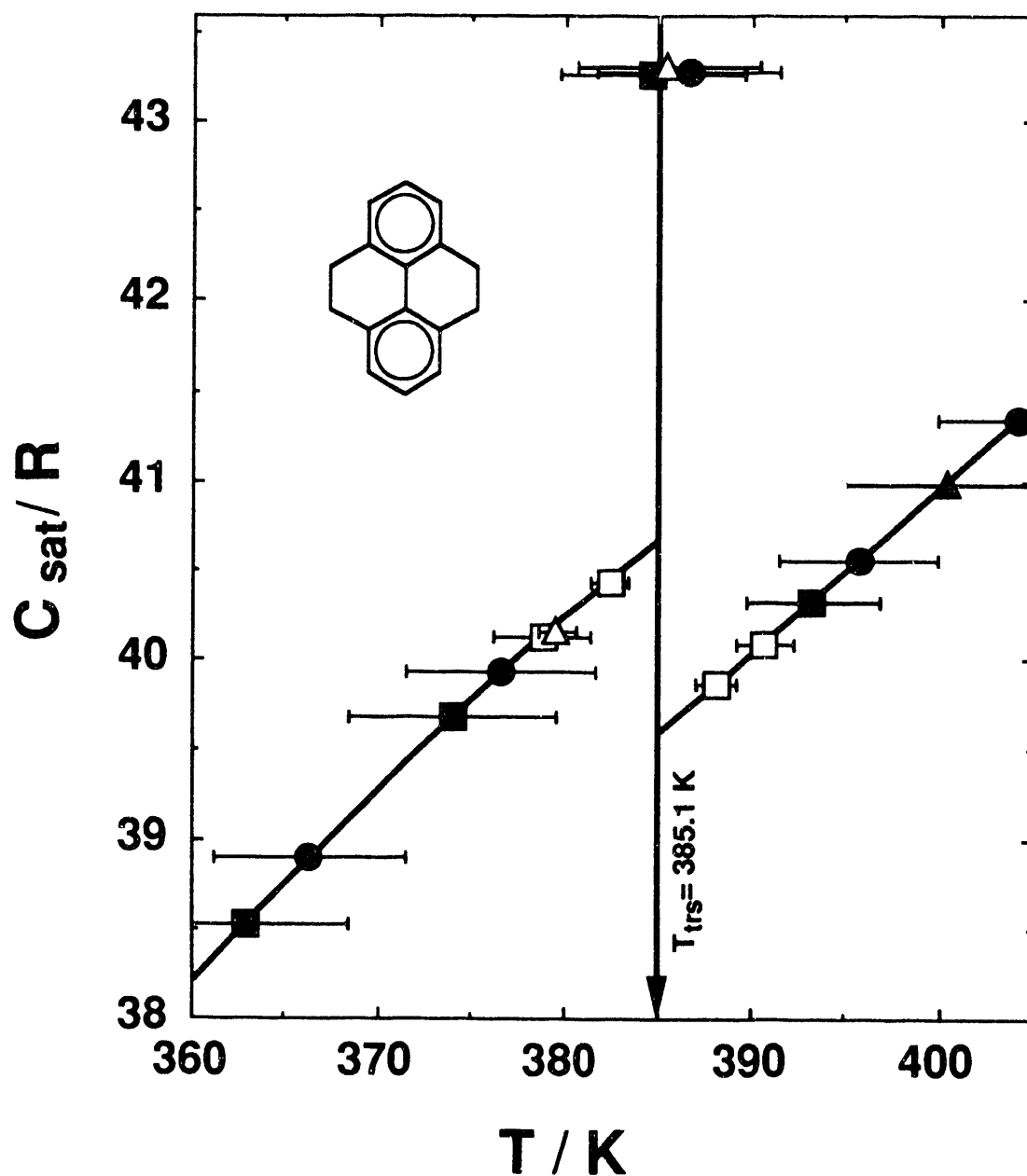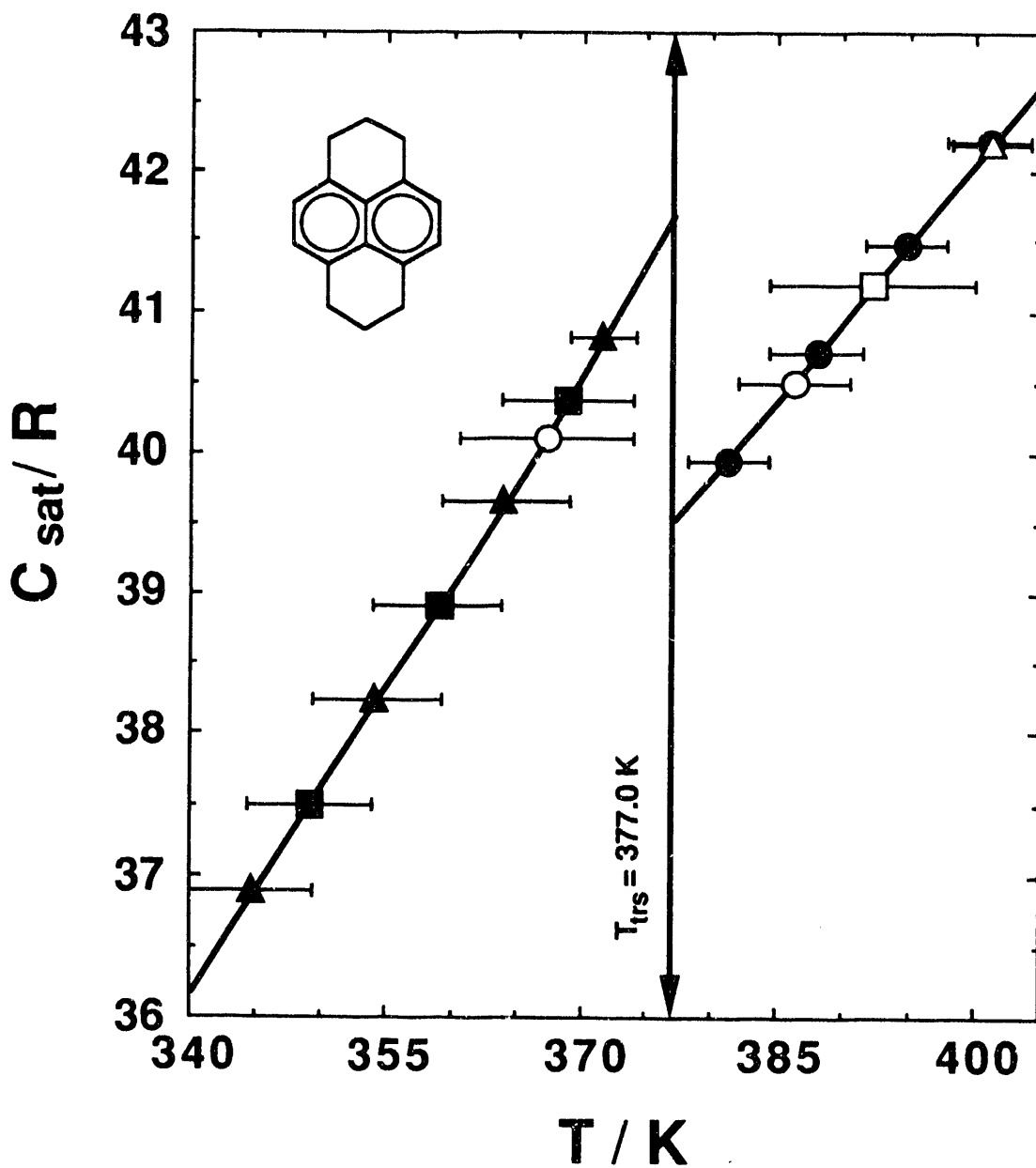
Figure 6. Average heat capacities in the cr(II)-to-cr(I) transition region for 1,2,3,6,7,8-hexahydropyrene. ●, Series 1; □, series 2; ▲, series 3; ○, series 4; ■, series 6; △, series 13. Results of measurements spanning T_{trs} (series 3, series 4, series 6, and series 12) are not shown. These are listed in table 9. The horizontal bars span the temperature increment associated with each average heat-capacity value. The vertical line indicates the phase-transition temperature. The heat-capacity curve is not defined uniquely between 374 K and 378 K. See text.

near the triple-point and solid-phase transition temperatures where equilibration times were long. The heat capacities for the crystal phases in table 10 have not been corrected for pre-melting. Pre-melting corrections[40] can be calculated with the temperature increments provided. Extrapolation of the heat-capacity results to $T \to 0$ for each compound was made by linear extrapolation of a plot of $C_{sat,m}/T$ against temperature squared for results below 10 K.

DIFFERENTIAL SCANNING CALORIMETRY

Theoretical Background. The theoretical background for the determination of heat capacities for the liquid phase at vapor-saturation pressure $C_{sat,m}$ with results obtained with a d.s.c. has been described.[34,41] If two phases are present and the liquid is a pure substance, then the vapor pressure p and the chemical potential μ are independent of the amount of substance n and the cell volume V_x, and are equal to p_{sat} and μ_{sat}. The two-phase heat capacities at cell volume V_x, $C_{x,m}^{II}$, can be expressed in terms of the temperature derivatives of these quantities:

$$n\, C_{x,m}^{II}/T \; = \; -n(\partial^2\mu/\partial T^2)_{sat} + V_x\,(\partial^2 p/\partial T^2)_{sat} + (\partial V_x/\partial T)_x(\partial p/\partial T)_{sat}. \qquad (7)$$

The third term on the right-hand side of equation (7) includes the thermal expansion of the cell. In this research the thermal expansion of the cells was expressed as:

$$V_x(T) \; / \; V_x(298.15 \text{ K}) \;\; = 1 + ay + by^2, \qquad (8)$$

where, $y = (T - 298.15)$ K, $a = 3.216 \times 10^{-5}$ K^{-1}, and $b = 5.4 \times 10^{-8}$ K^{-2}.

Values of $(\partial p/\partial T)_{sat}$ can be calculated based on the vapor pressures measured in this research. Therefore, with a minimum of two different filling levels of the cell, $(\partial^2 p/\partial T^2)_{sat}$ and $(\partial^2\mu/\partial T^2)_{sat}$ can be determined. In this research three fillings were used. To obtain the saturation heat capacity $C_{sat,m}$ at vapor pressures greater than 0.1 MPa, the limit where the cell is full of liquid is required; i.e., $(n/V_x) = \{1/V_m(l)\}$ where $V_m(l)$ is the molar volume of the liquid:

$$\lim_{(n/V_x) \to \{1/V_m(l)\}} (n\, C_{v,m}^{II}/T) \; = \;\; V_m(l)(\partial^2 p/\partial T^2)_{sat} - n(\partial^2\mu/\partial T^2)_{sat}. \qquad (9)$$

$C_{sat,m}$ is obtained from the expression:

$$\lim_{(n/V_x) \to \{1/V_m(l)\}} (n\, C_{v,m}^{II}) \; = \;\; n[C_{sat,m} - \{T(\partial p/\partial T)_{sat}\,(dV_m(l)/dT)\}]. \qquad (10)$$

Thus, reliable liquid-density values are also required to determine $C_{sat,m}$.

Measurement of Two-Phase (Liquid + Vapor) Heat Capacities. Table 9 lists the experimental two-phase heat capacities $C_{x,m}^{II}$ for 4,5,9,10-tetrahydropyrene and 1,2,3,6,7,8-hexahydropyrene obtained for three cell fillings for each compound. Heat capacities were determined at 20-K intervals with a heating rate of 0.083 K·s^{-1} and a 120-s equilibration period between heats. Sample decomposition precluded heat-capacity measurements above 745 K for both hydropyrenes.

For other compounds, e.g., 2-aminobiphenyl[42] and dibenzothiophene,[43] a rapid heating method was used for critical temperature and critical density determinations. By employing a single continuous heat at a rate of 0.333 K·s^{-1}, sample decomposition was greatly reduced, and the abrupt decrease in heat capacity associated with the conversion from two phases to one phase was observed. However, this method failed in the present research as there was extensive sample decomposition above the range of the heat-capacity measurements.

SIMULTANEOUS FITS TO VAPOR PRESSURES AND TWO-PHASE HEAT CAPACITIES

A simultaneous non-linear least-squares fit to the vapor pressures listed in table 5 and the $C_{x,m}^{II}$ values given in table 9 was completed as follows. The Wagner equation,[44] as formulated by Ambrose,[45] was used to represent the vapor pressures:

$$\ln(p/p_c) = (1/T_r)[A(1-T_r) + B(1-T_r)^{1.5} + C(1-T_r)^{2.5} + D(1-T_r)^5] , \qquad (11)$$

where $T_r = T/T_c$. The vapor-pressure fitting procedure resembled that used previously, when the Cox vapor-pressure equation was used.[16,29] In fits using the Wagner equation, the sums of the weighted squares in the following expression were minimized {replacing equation (12) of reference 16}:

$$\Delta = [\ln(p/p_c)/(1/T_r)] - A(1-T_r) - B(1-T_r)^{1.5} - C(1-T_r)^{2.5} - D(1-T_r)^5 . \qquad (12)$$

The weighting factors were derived with equation (13) of reference 16.

Experimental $C_{x,m}^{II}$ values were converted to $C_{v,m}^{II}$ by means of equation (8) for the cell expansion and the vapor-pressure fit for $(\partial p/\partial T)_{sat}$.

$$C_{v,m}^{II} = C_{x,m}^{II} - T/n \{(\partial V_x/\partial T)_x (\partial p/\partial T)_{sat}\}. \qquad (13)$$

The values of $C_{v,m}^{II}$ were used to derive functions for $(\partial^2 p/\partial T^2)_{sat}$ and $(\partial^2\mu/\partial T^2)_{sat}$. The functional form chosen for variation of the second derivative of the chemical potential with temperature was:

$$(\partial^2\mu/\partial T^2)_{sat} / (J \cdot K^{-2} \cdot mol^{-1}) = \sum_{i=0}^{n} b_i(1 - T/T_c)^i. \qquad (14)$$

{For compounds where sufficient information was available to evaluate reliably $(\partial^2\mu/\partial T^2)_{sat}$ (e.g., benzene[46]), four terms (i.e., expansion to n=3) were required to represent the function. Thus, four terms were used in this research.} In these fits the sum of the weighted squares in the following function was minimized:

$$\Delta = C_{v,m}^{II}/R - \{V_m(l)T/nR\}(\partial^2 p/\partial T^2)_{sat} + (T/R)(\partial^2\mu/\partial T^2)_{sat}. \qquad (15)$$

Within the heat-capacity results, the weighting factors were proportional to the square of the mass of sample used in the measurements. A weighting factor of 20 was used to increase the relative weights of the vapor-pressure measurements in the fit. The weighting factor reflects the higher precision of the vapor-pressure values relative to the experimental heat capacities obtained by d.s.c.

Estimation of Critical Temperatures. The fits were repeated for a range of fixed T_c values with the critical pressure included as a variable. The T_c values listed in table 10 for the hydropyrenes were selected to optimize agreement between the measured densities listed in table 2 and values calculated with the extended corresponding-states equation of Riedel,[47] as formulated by Hales and Townsend:[18]

$$(\rho/\rho_c) = 1.0 + 0.85\{1.0 - (T/T_c)\} + (1.692 + 0.986\omega)\{1.0 - (T/T_c)\}^{1/3}. \qquad (16)$$

Agreement between the measured and calculated values is indicated by a near-zero slope on a plot of their fractional differences with temperature. The critical density ρ_c was subsequently adjusted to minimize absolute differences. Figure 7 is a plot of fractional differences against temperature for 4,5,9,10-tetrahydropyrene for several values of T_c. The uncertainty in the selected critical temperature for each compound was estimated to be ± 5 K. All of the measured densities are within 0.1 per cent of values calculated with equation (16) and the selected critical properties, as shown in table 2 and figure 7.
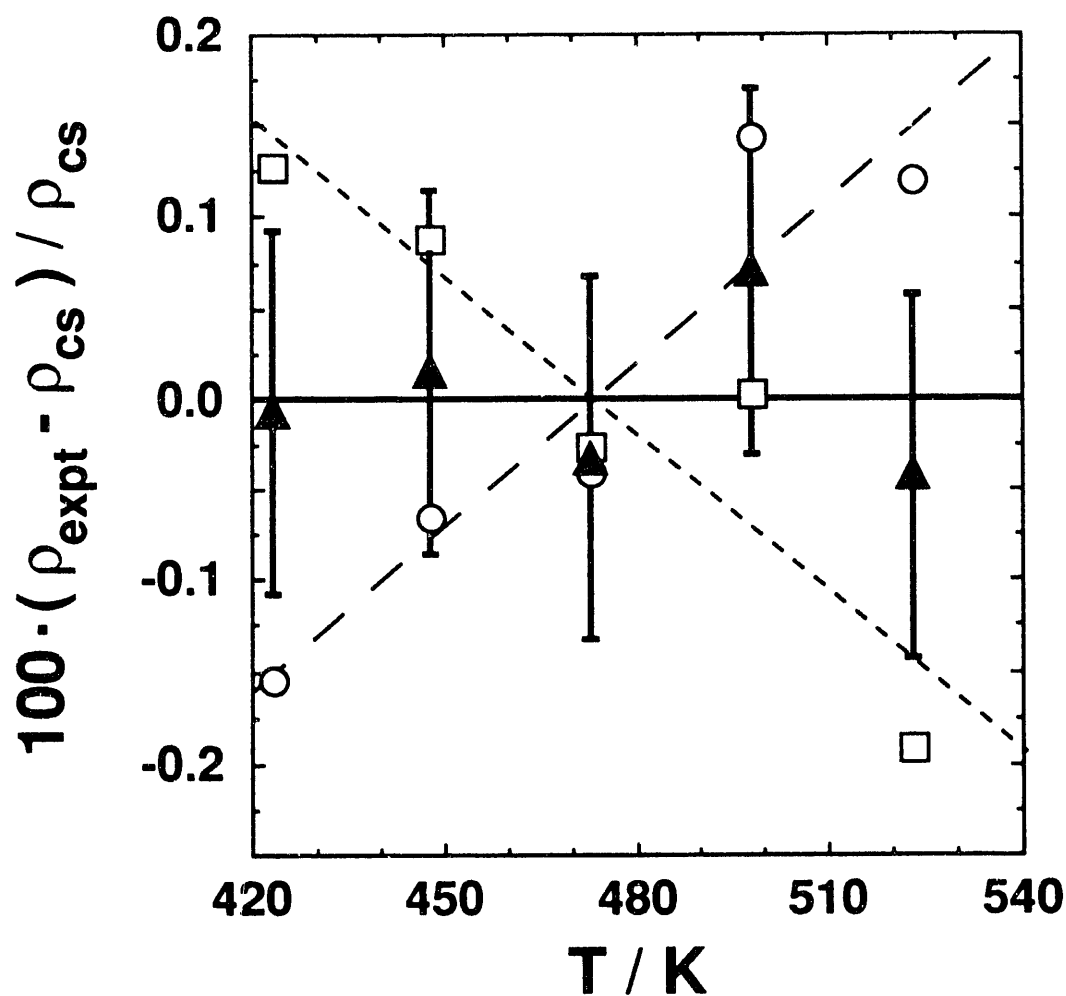
Figure 7. Deviation of measured densities ρ_{expt} for 4,5,9,10-tetrahydropyrene from values calculated with corresponding states ρ_{cs} {equation (16)} for several values of the critical temperature T_c. $\square$, T_c = 920 K; $\blacktriangle$, T_c = 900 K; $\bigcirc$, T_c = 880 K. The short dashes represent a straight-line fit to the results for T_c = 920 K; long dashes, T_c = 880 K; and uninterrupted line, T_c = 900 K. The error bars represent the estimated uncertainties in the measured densities.

Table 10 lists the coefficients determined in the non-linear least-squares fit. Deviations of the measured vapor pressures from the fitted Wagner equation are included in table 5. Values of $C_{sat,m}$ for 4,5,9,10-tetrahydropyrene and 1,2,3,6,7,8-hexahydropyrene were derived with equation (10) from $C_{v,m}^{II}(\rho = \rho_{sat})$ with densities obtained with equation (16). The results for $C_{v,m}^{II}(\rho = \rho_{sat})/R$ and $C_{sat,m}/R$ are reported in table 11. The estimated uncertainty in these values is 1 per cent. Differences between $C_{v,m}^{II}(\rho = \rho_{sat})/R$ and $C_{sat,m}/R$ are significant only at the highest temperatures measured. Differences in these quantities can be large as the critical temperature is approached.[41]

Derived Enthalpies of Vaporization. Enthalpies of vaporization $\Delta_l^g H_m$ were derived from the Wagner-equation fits by means of the Clapeyron equation:

$$dp/dT = \Delta_l^g H_m / (T \, \Delta_l^g V_m).\qquad(17)$$

$\Delta_l^g V_m$ is the increase in molar volume from the liquid to the real vapor. The Wagner-equation fits were employed to derive dp/dT. Estimates of liquid-phase volumes were made with equation (16) with $\rho_c = 324.3\ kg \cdot m^{-3}$, $T_c = 900\ K$, and acentric factor $\omega = 0.471$ for 1,2,3,4-tetrahydropyrene, and $\rho_c = 313.7\ kg \cdot m^{-3}$, $T_c = 920\ K$, and acentric factor $\omega = 0.513$ for 1,2,3,6,7,8-hexahydropyrene. The uncertainty in the liquid-phase volumes was estimated to be 1 per cent. [The acentric factor is defined as $\{-lg(p/p_c)-1\}$, where p is the vapor pressure at $T_r = 0.7$ and p_c is the critical pressure.] The Wagner-equation parameters given in table 13 were used to calculate p.

Vapor-phase volumes were calculated with the virial equation of state truncated at the third virial coefficient. Second virial coefficients were estimated with the corresponding-states equation of Pitzer and Curl,[48] and third virial coefficients were estimated with the corresponding-states method of Orbey and Vera.[49] This formulation for third virial coefficients was applied successfully in analyses of the thermodynamic properties of benzene, toluene, and decane.[50] Third virial coefficients are required for accurate calculation of the gas volume for pressures greater than 1 bar. Uncertainties in the virial coefficients are assumed to be 10 per cent. Derived enthalpies of vaporization are reported in table 12. For p>1 bar the uncertainties in the virial coefficients are the dominant contributions to the uncertainties in the derived enthalpies of vaporization. The effect of the ±5 K uncertainty in the critical temperatures was included in the uncertainty calculations. The effect is negligible below

500 K, but increases to approximately 20 per cent of the total uncertainty in the enthalpy of vaporization near 700 K.

THERMODYNAMIC PROPERTIES IN THE CONDENSED STATE

Entropies and enthalpies under vapor saturation pressure relative to that of the crystals at $T \rightarrow 0$ for the solid and liquid phases of 4,5,9,10-tetrahydropyrene and 1,2,3,6,7,8-hexahydropyrene are listed in table 13. The tabulated values were derived by integration of the smoothed heat capacities corrected for pre-melting, together with the entropies and enthalpies of transition and fusion. The heat capacities were smoothed with cubic-spline functions by least-squares fits to six points at a time and by requiring continuity in value, slope, and curvature at the junction of successive cubic functions. Due to limitations in the spline-function procedure, some acceptable values from tables 8 and 11 were not included in the fit, while in other regions graphical values were introduced to ensure that the second derivative of the heat capacity with respect to temperature was a smooth function of temperature. Pre-melting corrections were made by means of standard methods[40] for solid-insoluble impurities and the mole-fraction impurities values shown in table 1.

THERMODYNAMIC PROPERTIES IN THE IDEAL-GAS STATE

Enthalpies and entropies at selected temperatures for the ideal gas were calculated using values in tables 12 and 13 and are listed in columns 2 and 4 of table 14. Entropies and enthalpies of compression to 101.325 kPa were calculated based on the virial equation truncated after the third virial coefficient:

$$pV_m = RT + Bp + C'p^2 . \tag{18}$$

Formulations used to calculate the entropy and enthalpy of compression are:[51]

$$\Delta S_{comp,m} = R \ln(p) + (dB/dT)p + (dC'/dT)p^2 , \tag{19}$$

$$\Delta H_{comp,m} = \{B - T(dB/dT)\}p + \{C' - T(dC'/dT)\}(p^2/2). \tag{20}$$

Equations (19) and (20) are derived from equations (16.21) and (16.27), respectively, of reference 51. Temperature derivatives were estimated by numerical differentiation of virial coefficients estimated by the methods of Pitzer and Curl[48] and Orbey and Vera.[49]

   The first term in equation (19) is the entropy of compression, if the gas were ideal. The uncertainty in this term is not significant. The sum of the second and third

terms of equation (**19**) is the "gas-imperfection correction" to the entropy of compression. Equation (**20**) gives the "gas-imperfection correction" to the enthalpy of compression directly, as the ideal-gas value is zero. The gas-imperfection corrections are listed in table 14. Uncertainties in these values are difficult to assess because temperature derivatives of estimated values are involved. An uncertainty of 10 per cent of the calculated correction was assumed.

The derived ideal-gas enthalpies and entropies for 4,5,9,10-tetrahydropyrene and 1,2,3,6,7,8-hexahydropyrene were combined with the condensed-phase enthalpies of formation given in table 4 to calculate the enthalpies, entropies, and Gibbs energies of formation listed in columns 6, 7, and 8, respectively, of table 14.

Enthalpies and entropies for equilibrium hydrogen were determined from JANAF tables.[52] Values for graphite were determined with the polynomial[53] used to calculate the values from 298.15 K to 6000 K listed in the JANAF tables. All uncertainties in table 14 represent one standard deviation and do not include uncertainties in the properties of the elements.

CALCULATION OF SUBLIMATION PRESSURES

The "third-law" method was employed to calculate sublimation pressures for 4,5,9,10-tetrahydropyrene and 1,2,3,6,7,8-hexahydropyrene from 380 K to the triple-point temperatures. The "third-law" values were calculated from the tabulated thermodynamic functions of the ideal gas (table 14) and the crystalline solid (table 13). The method applied here was the same as that used previously for biphenyl.[41] The sublimation vapor pressures for 4,5,9,10-tetrahydropyrene were represented by the equation:

$$\ln(p/p^o) = 29.9515 - 9920.1(T/K)^{-1} - 1.9050 \times 10^5(T/K)^{-2}, \qquad (21)$$

in the temperature region 390 K to 412.725 K with p^o = 1 Pa. For 1,2,3,6,7,8-hexahydropyrene:

$$\ln(p/p^o) = 29.528 - 9517.6(T/K)^{-1} - 3.2394 \times 10^5(T/K)^{-2}, \qquad (22)$$

in the temperature region 380 K to 407.635 K.

4. DISCUSSION

COMPARISON OF RESULTS WITH LITERATURE

The property-measurement results reported here for 4,5,9,10-tetrahydropyrene and 1,2,3,6,7,8-hexahydropyrene are the first for these important intermediates in the pyrene/H_2 hydrogenation reaction network. A search of the literature (Chemical Abstracts; 1907 through 1991) failed to locate any previous thermodynamic-property measurements on these materials.

Sublimation pressures for phase cr(I) of 4,5,9,10-tetrahydropyrene and 1,2,3,6,7,8-hexahydropyrene were obtained as part of the inclined-piston vapor-pressure measurements. The measured values are reported in table 5 and marked by footnotes. Table 15 lists the measured sublimation pressures, liquid vapor pressures calculated with the Wagner equation parameters listed in table 10, and sublimation pressures calculated by means of the "third law" method {equations (21) and (22)}. The difference between the measured and calculated sublimation pressures (column 5 of table 15) for 1,2,3,6,7,8-hexahydropyrene are all within the expected uncertainty {0.2 Pa, per equation (4)} for the inclined-piston measurements. For 4,5,9,10-tetrahydropyrene the differences are slightly larger (roughly 0.5 Pa) near the triple-point temperature. The deviation probably arises from incomplete outgassing of the system during the inclined-piston measurements. This illustrates the difficulty in making low-pressure measurements in a static system, even when special outgassing techniques are used.

5. SUMMARY and HIGHLIGHTS

- Thermochemical and thermophysical properties for 4,5,9,10-tetrahydropyrene and 1,2,3,6,7,8-hexahydropyrene are reported. Properties measured included vapor pressures, heat capacities, and densities over a range of temperatures, and the energy of combustion.

- Ideal-gas thermodynamic properties for 4,5,9,10-tetrahydropyrene and 1,2,3,6,7,8-hexahydropyrene were determined based on the accurate calorimetric measurements.

- Gibbs energies of formation for 4,5,9,10-tetrahydropyrene and 1,2,3,6,7,8-hexahydropyrene for equilibria calculations were derived. The determination of these is an essential precursor to a thermodynamic analysis of hydrogen shuttling reactions, which is presented in a companion topical report.

- The first results of measurements with a new high-temperature densitometer were reported.

- The new density measurements were shown to provide key information for the accurate estimation of critical properties for materials, which decompose far below their critical temperatures. Critical temperatures for tetrahydro- and hexahydropyrene were estimated to be 900 K and 920 K, respectively, with an uncertainty of only ±5 K, even though the compounds decomposed nearly 200 K lower.

6. REFERENCES

1. Girgis, M. J.; Gates, B. C. *Ind. Eng. Chem. Res.* **1991**, 30, 2021.
2. Fisher, I. P.; Wilson, M. F. *Energy & Fuels* **1988**, 2, 548.
3. Cugini, A. V.; Lett, R. G.; Wender, I. *Energy & Fuels* **1989**, 3, 120.
4. Fouda, S. A.; Kelley, J. F.; Rahimi, P. M. *Energy & Fuels* **1989**, 3, 154.
5. Derbyshire, F. J.; Varghese, P.; Whitehurst, D. D. *Fuel* **1982**, 61, 859.
6. Mochida, I.; Yufu, A.; Sakanishi, K.; Korai, Y. *Fuel* **1988**, 67, 114.
7. Clarke, J. W.; Rantell, T. D.; Snape, C. E. *Fuel* **1984**, 63, 1476.
8. McMillan, D. F.; Malhotra, R.; Tse, D. S. *Energy & Fuels* **1991**, 5, 179.
9. Shaw, J. M.; Gaikwad, R. P.; Stowe, D. A. *Fuel* **1988**, 67, 1554.
10. Ricon, J. M.; Angulo, R. *Fuel* **1986**, 65, 889.
11. Cassidy, P. J.; Grint, A.; Jackson, W. R.; Larkins, F. P.; Louey, M. B.; Rash, D.; Watkins, J. D. *Proceedings of the 1987 International Conference on Coal Science.* Elsevier: Amsterdam. **1989**, p. 223.
12. Commission on Atomic Weights and Isotopic Abundances. *Pure Appl. Chem.* **1983**, 55, 1101.
13. Cohen, E. R.; Taylor, B. N. *J. Phys. Chem. Ref. Data* **1988**, 17, 1795.
14. *Metrologia* **1969**, 5, 35.
15. McCrackin, F. L.; Chang, S. S. *Rev. Sci. Instrum.* **1975**, 46, 550.
16. Steele, W. V.; Archer, D. G.; Chirico, R. D.; Collier, W. B.; Hossenlopp, I. A.; Nguyen, A.; Smith, N. K.; Gammon, B. E. *J. Chem. Thermodynamics* **1988**, 20, 1233.
17. Haar, L.; Gallagher, J. S.; Kell, G. S. *NBS/NRC Steam Tables* Hemisphere: Washington DC. **1984**.
18. Hales, J. L.; Townsend, R. *J. Chem. Thermodynamics* **1972**, 4, 763.
19. Good, W. D.; Moore, R. T. *J. Chem. Eng. Data* **1970**, 15, 150.
20. Good, W. D.; Smith, N. K. *J. Chem. Eng. Data* **1969**, 14, 102.
21. Good, W. D. *J. Chem. Eng. Data* **1969**, 14, 231.
22. Good, W. D.; Scott, D. W.; Waddington, G. *J. Phys. Chem.* **1956**, 60, 1080.
23. Good, W. D.; Douslin, D. R.; Scott, D. W.; George, A.; Lacina, J. L.; McCullough, J. P.; Waddington, G. *J. Phys. Chem.* **1959**, 63, 1133.
24. Smith, N. K.; Stewart, R. C., Jr.; Osborn, A. G.; Scott, D. W. *J. Chem. Thermodynamics* **1980**, 12, 919.
25. Chirico, R. D.; Hossenlopp, I. A.; Nguyen, A.; Strube, M. M.; Steele, W. V. *Thermodynamic Studies Related to the Hydrogenation of Phenanthrene.* NIPER-247. Published by DOE Fossil Energy, Bartlesville Project Office. Available from NTIS Report No. DE-87001252, April **1987**.
26. Goldberg, R. N.; Nuttall, R. N.; Prosen, E. J.; Brunetti, A. P. *NBS Report 10437,* U. S. Department of Commerce, National Bureau of Standards, June **1971**.
27. Swietoslawski, W. *Ebulliometric Measurements.* Reinhold: New York. **1945**.
28. Osborn A. G.; Douslin, D. R. *J. Chem. Eng. Data* **1966**, 11, 502.
29. Chirico, R. D.; Nguyen, A.; Steele, W. V.; Strube, M. M.; Tsonopoulos, C. *J. Chem. Eng. Data* **1989**, 34, 149.
30. Antoine, C. *C. R. Acad. Sci.* **1888**, 107, 681.
31. Douslin, D. R.; McCullough, J. P. *U. S. Bureau of Mines. Report of Investigation 6149,* **1963**, pp. 11.

32. Douslin, D. R.; Osborn A. G. *J. Sci. Instrum.* **1965**, 42, 369.

33. Steele, W. V.; Chirico, R. D.; Knipmeyer, S. E.; Smith, N. K. *High-Temperature Heat-Capacity Measurements and Critical Property Determinations using a Differential Scanning Calorimeter. (Development of Methodology and Application to Pure Organic Compounds)* NIPER-360, December **1988**. Published by DOE Fossil Energy, Bartlesville Project Office. Available from NTIS Report No. DE88000709.

34. Knipmeyer, S. E.; Archer, D. G.; Chirico, R. D.; Gammon, B. E.; Hossenlopp, I. A.; Nguyen, A.; Smith, N. K.; Steele, W. V.; Strube, M. M. *Fluid Phase Equilibria* **1989**, 52, 185.

35. Mraw, S. C.; Naas, D. F. *J. Chem. Thermodynamics* **1979**, 11, 567.

36. Hubbard, W. N.; Scott, D. W.; Waddington, G. *Experimental Thermochemistry.* Rossini, F. D.: editor. Interscience: New York. **1956**. Chap. 5, pp. 75-128.

37. Smith, N. K.; Good, W. D. *J. Chem. Eng. Data* **1967**, 12, 572.

38. Rossini, F. D. *Experimental Thermochemistry.* Rossini, F. D.: editor. Interscience: New York. **1956**. Chap. 14, pp. 297-320.

39. Cox, J. D.; Wagman, D. D.; Medvedev, V. A.: editors. *CODATA Key Values for Thermodynamics.* Hemisphere: New York. **1989**.

40. Westrum, E. F., Jr.; Furukawa, G. T.; McCullough, J. P. *Experimental Thermodynamics.* Vol. 1. McCullough, J. P.; Scott, D. W.: editors. Butterworths: London. **1968**. Chap 5.

41. Chirico, R. D.; Knipmeyer, S. E.; Nguyen, A.; Steele, W. V. *J. Chem. Thermodynamics* **1989**, 21, 1307.

42. Steele, W. V.; Chirico, R. D.; Knipmeyer, S. E.; Nguyen, A. *J. Chem. Thermodynamics* **1991**, 23, 957.

43. Chirico, R. D.; Knipmeyer, S. E.; Nguyen, A.; Steele, W. V. *J. Chem. Thermodynamics* **1991**, 23, 431.

44. Wagner, W, Cryogenics **1973**, 13, 470.

45. Ambrose, D.; Ewing, M. B.; Ghiassee, N. B.; Sanchez Ochoa, J. C. *J. Chem. Thermodynamics* **1990**, 22, 589.

46. Goodwin, R. D. *J. Phys. Chem. Ref. Data* **1988**, 17, 1541.

47. Riedel, L. *Chem.-Ing.-Tech.* **1954**, 26, 259.

48. Pitzer, K. S.; Curl, R. F. Jr. *J. Am. Chem. Soc.* **1957**, 79, 2369.

49. Orbey, H.; Vera, J. H. *AIChE J.,* **1983**, 29, 107.

50. Steele, W. V.; Chirico, R. D. To be published.

51. Lewis, G. N.; Randall, M. *Thermodynamics.* Revised by Pitzer, K. S.; Brewer, L. 2nd edition. McGraw-Hill: New York. **1961**.

52. Chase, M. W., Jr.; Davies, C. A.; Downey, J. R.; Frurip, D. J.; McDonald, R. A.; Syverud, A. N. *JANAF Thermochemical Tables* Third edition. Supplement to *J. Phys. Chem. Ref. Data* **1985**, 14.

53. Chirico, R. D.; Archer, D. G.; Hossenlopp, I. A.; Nguyen, A.; Steele, W. V.; Gammon, B. E. *J. Chem. Thermodynamics* **1990**, 22, 665.

TABLE 1. Calorimeter and sample characteristics for adiabatic heat-capacity calorimetry studies: m is the sample mass; V_i is the internal volume of the calorimeter; T_{cal} is the temperature of the calorimeter when sealed; p_{cal} is the pressure of the helium and sample when sealed; r is the ratio of the heat capacity of the full calorimeter to that of the empty; T_{max} is the highest temperature of the measurements; and $\delta C/C$ is the vaporization correction; x_{pre} is the mole-fraction impurity used for pre-melting corrections
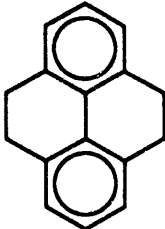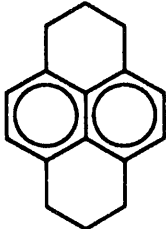
	4,5,9,10-Tetrahydropyrene	1,2,3,6,7,8-Hexahydropyrene
m/g	41.537	39.192
$V_i(298.15\ K)/cm^3$	61.0	59.06
T_{cal}/K	298.0	298.0
p_{cal}/kPa	8.07	7.23
$r(T_{max})$	3.1	2.8
r_{min}	1.5	1.5
$10^2 \cdot (\delta C/C)_{max}$	0.036	0.004
x_{pre}	0.00005	0.00031

TABLE 2. Measured density values at saturation pressure [a]

T/K	$\rho/(kg \cdot m^{-3})$	$100 \cdot (\rho - \rho_{cs})/\rho$	T/K	$\rho/(kg \cdot m^{-3})$	$100 \cdot (\rho - \rho_{cs})/\rho$
	4,5,9,10-Tetrahydropyrene			1,2,3,6,7,8-Hexahydropyrene	
423.15	1036.2	−0.01	423.15	1018.6	−0.04
448.15	1018.7	0.01	448.15	1002.2	0.00
473.15	1000.1	−0.03	473.15	984.9	−0.01
498.15	982.6	0.07	498.15	968.3	0.08
523.15	962.5	−0.04	523.15	949.2	−0.03

[a] ρ_{cs} = density calculated using extended corresponding states. {See equation (16) and text.}

TABLE 3. Typical combustion experiments at 298.15 K [a] (p° = 101.325 kPa)

	4,5,9,10-Tetrahydro-pyrene	1,2,3,6,7,8-Hexahydro-pyrene
m'(compound)/g	0.831591	0.818835
m'''(fuse)/g	0.001736	0.001691
$n_i(H_2O)$/mol	0.05535	0.05535
$m(Pt)$/g	19.971	19.971
$\Delta T/K$ =(t_i − t_f + Δt_{corr})/K	1.99901	1.99973
ε(calor)(ΔT)/J	−33526.5	−33538.5
ε(cont)(ΔT)/J [b]	−36.5	−36.3
ΔU_{ign}/J	0.8	0.8
ΔU(corr. to std. states)/J [c]	19.3	18.1
$-m'''(\Delta_c U^o_m/M)$(fuse)/J	29.4	28.7
$m'(\Delta_c U^o_m/M)$(compound)/J	−33513.5	−33527.2
$(\Delta_c U^o_m/M)$(compound)/J·g^{-1}	−40300.5	−40945.0

[a] The symbols and abbreviations of this Table are those of reference 36 except as noted.

[b] ε_i(cont)(t_i − 298.15 K) + ε_f(cont)(298.15 K − t_f + Δt_{corr})

[c] Items 81 to 85, 87 to 90, 93, and 94 of the computational form of reference 36.

TABLE 4. Summary of experimental energy of combustion results and molar thermodynamic functions. T = 298.15 K, and p° =101.325 kPa

4,5,9,10-Tetrahydropyrene

$\{(\Delta_c U_m^{\circ}/M)(4,5,9,10\text{-Tetrahydropyrene})\}/(J \cdot g^{-1})$

-40300.5	-40300.9	-40296.4	-40302.4	-40296.6	-40302.9

$<\{(\Delta_c U_m^{\circ}/M)(4,5,9,10\text{-Tetrahydropyrene})\}/(J \cdot g^{-1})>$	-40300.5±1.3
$(\Delta_c U_m^{\circ})(4,5,9,10\text{-Tetrahydropyrene})/(kJ \cdot mol^{-1})$	-8313.50±1.21
$(\Delta_c H_m^{\circ})(4,5,9,10\text{-Tetrahydropyrene})/(kJ \cdot mol^{-1})$	-8322.18±1.21
$(\Delta_f H_m^{\circ})(4,5,9,10\text{-Tetrahydropyrene})/(kJ \cdot mol^{-1})$	25.21±1.46

1,2,3,6,7,8-Hexahydropyrene

$\{(\Delta_c U_m^{\circ}/M)(1,2,3,6,7,8\text{-Hexahydropyrene})\}/(J \cdot g^{-1})$

-40945.0	-40942.8	-40955.4	-40949.9	-40936.4	-40935.2

$<\{(\Delta_c U_m^{\circ}/M)(1,2,3,6,7,8\text{-Hexahydropyrene})\}/(J \cdot g^{-1})>$	-40944.2±3.2
$(\Delta_c U_m^{\circ})(1,2,3,6,7,8\text{-Hexahydropyrene})/(kJ \cdot mol^{-1})$	-8528.83±1.74
$(\Delta_c H_m^{\circ})(1,2,3,6,7,8\text{-Hexahydropyrene})/(kJ \cdot mol^{-1})$	-8538.75±1.74
$(\Delta_f H_m^{\circ})(1,2,3,6,7,8\text{-Hexahydropyrene})/(kJ \cdot mol^{-1})$	-44.05±1.92

TABLE 5. Vapor-pressure results: IP refers to measurements performed with the inclined-piston gauge; water or decane refers to which material was used as the standard in the reference ebulliometer; T is the temperature of the experimental inclined-piston pressure gauge measurements or, for ebulliometric measurements, of the condensation temperature of the sample; the pressure p for ebulliometric measurements was calculated from the condensation temperature of the reference substance; Δp is the difference of the value of pressure calculated using the Wagner vapor pressure equation from the observed value of pressure; $\sigma(p)$ is the propagated error calculated from equations (3) and (4); ΔT is the difference between the boiling and condensation temperatures $(T_{boil} - T_{cond})$ for the sample in the ebulliometer

Method	$\dfrac{T}{K}$	$\dfrac{p}{kPa}$	$\dfrac{\Delta p}{kPa}$	$\dfrac{\sigma(p)}{kPa}$	$\dfrac{\Delta T}{K}$
		4,5,9,10-Tetrahydropyrene			
IP	385.000 [a,b]	0.0183		0.0002	
IP	390.001 [a,b]	0.0262		0.0002	
IP	395.002 [a,b]	0.0373		0.0002	
IP	405.003 [a,b]	0.0740		0.0002	
IP	410.002 [a,b]	0.1022		0.0002	
IP	425.000	0.2231	0.0000	0.0002	
IP	434.996	0.3555	0.0000	0.0003	
IP	445.002	0.5526	0.0000	0.0003	
IP	455.000	0.8386	-0.0002	0.0003	
IP	465.002	1.2457	-0.0002	0.0004	
IP	475.001	1.8134	-0.0001	0.0005	
decane	477.696	2.0000	0.0000	0.0001	0.081
IP	485.002	2.5902	-0.0002	0.0006	
decane	485.833	2.6660	-0.0001	0.0002	0.061
IP	490.001	3.0754	0.0002	0.0007	
decane	497.909	3.9999	0.0004	0.0002	0.060
decane	506.934	5.3330	0.0003	0.0003	0.056
decane	520.363	7.9989	-0.0001	0.0004	0.043
decane	530.444	10.6661	-0.0010	0.0005	0.039
decane	538.592	13.332	0.000	0.001	0.036
decane	547.059	16.665	0.000	0.001	0.032
decane	554.094	19.933	0.001	0.001	0.037

TABLE 5. Continued

Method	$\dfrac{T}{K}$	$\dfrac{p}{kPa}$	$\dfrac{\Delta p}{kPa}$	$\dfrac{\sigma(p)}{kPa}$	$\dfrac{\Delta T}{K}$
decane	563.360	25.023	0.000	0.001	0.034
water	563.360 [b]	25.023	-0.001	0.001	0.033
water	572.689	31.177	-0.002	0.002	0.032
water	582.073	38.565	0.003	0.002	0.028
water	591.526	47.375	0.002	0.002	0.025
water	601.039	57.817	0.003	0.003	0.025
water	610.622	70.120	-0.003	0.003	0.023
water	620.261	84.533	0.001	0.003	0.025
water	629.964	101.325	0.001	0.004	0.041
water	639.737	120.79	-0.01	0.01	0.044
water	649.556	143.25	0.01	0.01	0.069
water	659.515 [b]	169.02	-0.19	0.01	0.089

1,2,3,6,7,8-Hexahydropyrene

Method	$\dfrac{T}{K}$	$\dfrac{p}{kPa}$	$\dfrac{\Delta p}{kPa}$	$\dfrac{\sigma(p)}{kPa}$	$\dfrac{\Delta T}{K}$
IP	390.004 [a,b]	0.0201		0.0002	
IP	395.001 [a,b]	0.0287		0.0002	
IP	400.001 [a,b]	0.0409		0.0002	
IP	405.003 [a,b]	0.0576		0.0002	
IP	410.000	0.0778	-0.0001	0.0002	
IP	420.000	0.1304	0.0000	0.0002	
IP	430.002	0.2119	-0.0002	0.0002	
IP	440.001	0.3359	-0.0001	0.0003	
IP	450.005	0.5195	-0.0002	0.0003	
IP	460.004	0.7851	-0.0005	0.0003	
IP	459.997	0.7853	0.0000	0.0003	
IP	470.004	1.1624	-0.0003	0.0004	
IP	479.999	1.6870	-0.0001	0.0005	
decane	484.736	2.0000	0.0003	0.0001	0.064
IP	490.002	2.4045	0.0000	0.0006	
decane	493.015	2.6660	-0.0002	0.0002	0.050
IP	499.001	3.2591	0.0001	0.0007	
decane	505.295	3.9999	-0.0002	0.0002	0.038

35

TABLE 5. Continued

Method	$\dfrac{T}{K}$	$\dfrac{p}{kPa}$	$\dfrac{\Delta p}{kPa}$	$\dfrac{\sigma(p)}{kPa}$	$\dfrac{\Delta T}{K}$
decane	514.463	5.3330	−0.0001	0.0003	0.029
decane	528.097	7.9989	0.0000	0.0004	0.035
decane	538.326	10.6661	−0.0004	0.0005	0.035
decane	546.592	13.332	0.000	0.001	0.036
decane	555.178	16.665	0.000	0.001	0.034
decane	562.311	19.933	0.000	0.001	0.035
decane	571.696	25.023	0.000	0.001	0.031
water [b]	571.695	25.023	0.001	0.001	0.030
water	581.139	31.177	0.002	0.002	0.028
water	590.646	38.565	−0.001	0.002	0.023
water	600.205	47.375	−0.001	0.002	0.023
water	609.822	57.817	−0.001	0.003	0.024
water	619.497	70.120	−0.003	0.003	0.024
water	629.224	84.533	0.003	0.003	0.028
water	638.990 [b]	101.325	0.038	0.004	0.057

[a] Phase cr(l).
[b] The value at this temperature was not included in the fit.

TABLE 6. Melting-study summaries: F is the fraction melted at observed temperature
T(F); T_{tp} is the triple-point temperature; x is the mole-fraction impurity

F	T(F)/K	F	T(F)/K
4,5,9,10-Tetrahydropyrene		**1,2,3,6,7,8-Hexahydropyrene**	
0.150	412.670	0.154	407.557
0.300	412.692	0.253	407.586
0.400	412.699	0.402	407.604
0.600	412.707	0.601	407.615
0.800	412.711	0.801	407.620
T_{tp} = 412.725 K		T_{tp} = 407.635 K	
x = 0.00018		x = 0.00016	

TABLE 7. Molar enthalpy measurements $(R=8.31451 \; J \cdot K^{-1} \cdot mol^{-1})$

N^a	h^b	$\dfrac{T_i}{K}$	$\dfrac{T_f}{K}$	$\dfrac{T_{trs}}{K}$	$\dfrac{\Delta_{tot}U_m{}^c}{R \cdot K}$	$\dfrac{\Delta_{trs}H_m{}^d}{R \cdot K}$
			4,5,9,10-Tetrahydropyrene			
			Single-phase measurements in cr(III)			
10	1	212.447	274.114		1456.5	0.2
12	1	218.613	280.812		1513.3	0.3
13	1	222.212	285.310		1563.9	0.5
13	1	285.308	315.013		896.3	0.5
15	1	53.399	180.717		1442.9	0.1
15	1	180.732	304.287		2919.4	0.4
19	1	275.906	317.345		1232.1	−0.2
			cr(III) to cr(II)			
10	1	317.716	324.148	319.9	656.3	442.2
15	1	317.590	324.050		655.6	440.8
19	2	317.350	324.256		665.6	436.0 [e]
					Average:	441.5
			Single-phase measurements in cr(II)			
20	1	321.681	378.595		2107.5	0.4
			cr(II) to cr(I)			
2	1	381.699	391.508	385.1	424.6	31.3
4	2	383.460	387.107		177.3	31.1 [e]
5	1	379.628	389.648		433.6	31.4
20	1	380.594	390.399		424.7	31.4
					Average:	31.4
			Single-phase measurements in cr(I)			
21	1	387.806	407.719		811.2	−0.2

38

TABLE 7. Continued

N [a]	h [b]	$\dfrac{T_i}{K}$	$\dfrac{T_f}{K}$	$\dfrac{T_{trs}}{K}$	$\dfrac{\Delta_{tot}U_m}{R \cdot K}$ [c]	$\dfrac{\Delta_{trs}H_m}{R \cdot K}$ [d]
		cr(I) to liquid				
2	6	408.506	414.333	412.725	2307.3	2056.1
3	2	405.782	415.620		2480.3	2055.9
21	2	407.718	415.520		2394.8	2055.6
					Average:	2055.9
		Single-phase measurements in liquid				
23	1	428.113	507.720		4010.3	−0.4

1,2,3,6,7,8-Hexahydropyrene

N [a]	h [b]	$\dfrac{T_i}{K}$	$\dfrac{T_f}{K}$	$\dfrac{T_{trs}}{K}$	$\dfrac{\Delta_{tot}U_m}{R \cdot K}$ [c]	$\dfrac{\Delta_{trs}H_m}{R \cdot K}$ [d]
		Single-phase measurements in cr(II)				
11	1	72.571	201.275		1737.2	−0.1
11	1	201.274	322.330		3204.7	0.1
12	1	303.063	371.828		2470.7	−0.8
		cr(II) to cr(I)				
3	3	374.210	382.341	377.0	1529.3	1201.4 [e]
4	1	374.008	382.156		1528.9	1200.2
6	3	374.052	382.195		1527.4	1198.9 [e]
12	1	371.520	382.655		1650.9	1200.3
					Average:	1200.2
		Single-phase measurements in cr(I)				
6	1	382.167	400.833		767.3	0.0
12	1	382.638	403.307		853.0	−0.1

TABLE 7. Continued

N^a	h^b	$\dfrac{T_i}{K}$	$\dfrac{T_f}{K}$	$\dfrac{T_{trs}}{K}$	$\dfrac{\Delta_{tot}U_m}{R{\cdot}K}^c$	$\dfrac{\Delta_{trs}H_m}{R{\cdot}K}^d$
			cr(I) to liquid			
1	2	404.146	409.972	407.635	2433.7	2176.2
2	6	399.976	409.138		2571.6	2176.4
1 2	2	403.237	410.954		2517.5	2175.7
1 3	2	404.268	410.207		2439.2	2175.9
					Average:	2176.1

[a] Adiabatic series number.

[b] Number of heating increments.

[c] $\Delta_{tot}U_m$ is the molar energy input from the initial temperature T_i to the final temperature T_f.

[d] $\Delta_{trs}H_m$ is the net molar enthalpy of transition at the transition temperature T_{trs} or the excess enthalpy relative to the heat-capacity curve described in the text for single-phase measurements.

[e] This value was not included in the average.

TABLE 8. Molar heat capacities at vapor-saturation pressure ($R = 8.31451$ $J \cdot K^{-1} \cdot mol^{-1}$)

N^a	$\dfrac{<T>}{K}$	$\dfrac{\Delta T}{K}$	$\dfrac{C_{sat,m}^b}{R}$	N^a	$\dfrac{<T>}{K}$	$\dfrac{\Delta T}{K}$	$\dfrac{C_{sat,m}^b}{R}$
			4,5,9,10-Tetrahydropyrene				
			cr(III)				
14	5.212	1.0343	0.072	13	135.719	10.0435	12.897
14	6.190	0.9160	0.122	13	145.813	10.1414	13.810
14	7.150	0.9830	0.188	13	155.916	10.0598	14.740
14	8.150	1.0102	0.278	13	166.064	10.1938	15.695
14	9.173	1.0344	0.389	13	176.247	10.1693	16.669
14	10.223	1.0671	0.527	13	186.454	10.2396	17.665
14	11.358	1.2040	0.684	13	196.652	10.1545	18.681
14	12.634	1.3465	0.869	13	206.865	10.2648	19.720
14	14.045	1.4749	1.089	13	217.096	10.1938	20.773
14	15.606	1.6500	1.329	9	217.182	9.9332	20.775
14	17.339	1.8158	1.594	9	227.183	10.0549	21.840
14	19.248	2.0023	1.876	9	237.309	10.1774	22.927
14	21.354	2.2135	2.182	9	247.515	10.2214	24.052
14	23.675	2.4268	2.508	9	257.745	10.2170	25.197
14	26.220	2.6639	2.847	9	268.013	10.1645	26.362
14	29.044	2.9854	3.206	9	278.187	10.1668	27.540
14	32.183	3.2934	3.588	10	280.340	12.4333	27.785
14	35.669	3.6777	3.993	12	286.678	11.4509	28.525
14	39.571	4.1256	4.418	9	288.348	10.1243	28.728
14	43.912	4.5565	4.872	18	291.012	10.1138	29.029
14	48.749	5.1161	5.344	10	292.819	12.5149	29.261
14	54.167	5.7183	5.867	12	298.278	11.6561	29.916
13	54.439	4.4275	5.888	9	298.458	10.0823	29.948
13	59.440	5.5509	6.351	18	301.139	10.1203	30.253
14	60.187	6.3187	6.412	10	305.316	12.4644	30.731
13	65.342	6.2419	6.866	11	306.652	9.3531	30.943
13	71.914	6.8963	7.430	9	308.545	10.0759	31.137
13	79.202	7.6724	8.041	12	308.674	9.1113	31.190

TABLE 8. Continued

N[a]	$\dfrac{<T>}{K}$	$\dfrac{\Delta T}{K}$	$\dfrac{C_{sat,m}}{R}$ [b]	N[a]	$\dfrac{<T>}{K}$	$\dfrac{\Delta T}{K}$	$\dfrac{C_{sat,m}}{R}$ [b]
13	87.358	8.3831	8.726	15	310.935	13.1753	31.455
13	96.200	9.2971	9.471	18	311.269	10.1278	31.498
13	105.822	9.9396	10.288	10	314.620	6.0361	31.876
13	115.743	9.8975	11.138	11	315.405	8.0250	32.041
13	125.695	9.9995	12.007	12	316.057	5.6025	32.106

<div align="center">cr(II)</div>

N[a]	$\dfrac{<T>}{K}$	$\dfrac{\Delta T}{K}$	$\dfrac{C_{sat,m}}{R}$ [b]	N[a]	$\dfrac{<T>}{K}$	$\dfrac{\Delta T}{K}$	$\dfrac{C_{sat,m}}{R}$ [b]
5	292.069	8.9792	30.219	6	342.263	9.5754	36.147
5	301.535	9.9236	31.318	1	348.038	10.1291	36.835
17	303.871	9.8767	31.586	5	352.242	10.0933	37.340
5	311.539	10.0627	32.497	1	358.183	10.1663	38.005
5	321.655	10.1527	33.693	5	362.920	11.0953	38.527
19	328.175	7.8724	34.475	2	366.333	10.2492	38.899
16	330.937	10.2439	34.768	5	374.013	11.0261	39.677
5	331.932	10.2208	34.901	2	376.579	10.2458	39.937
6	332.598	9.7533	35.011	4	378.840	5.1406	40.133
1	337.924	10.1022	35.614	20	379.595	1.9943	40.159
5	342.114	10.1283	36.145	4	382.435	2.0449	40.431

<div align="center">cr(I)</div>

N[a]	$\dfrac{<T>}{K}$	$\dfrac{\Delta T}{K}$	$\dfrac{C_{sat,m}}{R}$ [b]	N[a]	$\dfrac{<T>}{K}$	$\dfrac{\Delta T}{K}$	$\dfrac{C_{sat,m}}{R}$ [b]
4	388.144	2.0636	39.872	2	395.723	8.4464	40.582
4	390.724	3.0893	40.103	3	400.382	10.8183	41.056
5	393.272	7.1842	40.340	2	404.234	8.6005	41.503

<div align="center">liquid</div>

N[a]	$\dfrac{<T>}{K}$	$\dfrac{\Delta T}{K}$	$\dfrac{C_{sat,m}}{R}$ [b]	N[a]	$\dfrac{<T>}{K}$	$\dfrac{\Delta T}{K}$	$\dfrac{C_{sat,m}}{R}$ [b]
2	418.412	8.1641	46.599	22	454.289	18.1170	49.392
21	419.516	7.9890	46.682	22	472.292	17.8370	50.721
3	420.606	9.9752	46.770	22	490.010	17.5722	52.027
3	430.527	9.8782	47.557	22	506.509	15.4167	53.205
22	435.172	20.4911	47.918	22	518.508	8.5939	54.030
3	440.456	9.9883	48.332				

TABLE 8. Continued

N^a	$\dfrac{<T>}{K}$	$\dfrac{\Delta T}{K}$	$\dfrac{C_{sat,m}{}^b}{R}$	N^a	$\dfrac{<T>}{K}$	$\dfrac{\Delta T}{K}$	$\dfrac{C_{sat,m}{}^b}{R}$

1,2,3,6,7,8-Hexahydropyrene

cr(II)

N^a	$<T>$	ΔT	$C_{sat,m}$	N^a	$<T>$	ΔT	$C_{sat,m}$
10	6.620	1.2404	0.072	8	129.333	9.7483	12.718
10	7.737	0.9044	0.113	8	139.182	9.9309	13.629
10	8.713	0.9778	0.167	8	149.085	9.8500	14.549
10	9.702	0.9993	0.232	8	159.080	9.8995	15.513
10	10.766	1.1287	0.320	8	169.024	9.9676	16.468
10	11.954	1.2418	0.434	8	179.003	9.9656	17.445
10	13.269	1.3910	0.577	8	189.016	10.0259	18.446
10	14.804	1.6815	0.757	8	199.088	10.0939	19.466
10	16.494	1.6957	0.980	8	209.175	10.0599	20.506
10	18.301	1.9211	1.236	8	219.260	10.0304	21.571
10	20.326	2.1259	1.528	8	229.365	10.0304	22.662
10	22.575	2.3681	1.860	7	234.206	11.5935	23.197
10	25.090	2.6639	2.230	8	239.484	10.0316	23.783
10	27.904	2.9632	2.633	7	245.137	10.2465	24.411
10	31.020	3.2691	3.068	7	255.375	10.1969	25.588
10	34.469	3.6298	3.535	7	265.514	10.0567	26.761
10	38.287	4.0073	4.023	7	275.635	10.1395	27.961
10	42.508	4.4350	4.533	7	285.874	10.2165	29.206
10	47.173	4.8937	5.068	7	296.123	10.2689	30.481
10	52.372	5.5060	5.629	7	306.287	10.0415	31.762
9	57.959	6.5571	6.217	7	316.307	9.9851	33.054
11	58.625	5.5408	6.294	7	326.281	9.9536	34.369
11	63.942	5.0716	6.790	3	335.328	9.2106	35.578
9	64.278	6.0476	6.817	7	336.246	9.9671	35.706
11	69.504	6.0458	7.328	3	344.777	9.4546	36.889
9	70.703	6.7762	7.435	6	349.252	9.8046	37.493
9	77.980	7.4310	8.097	3	354.365	9.6930	38.248
9	85.745	8.0785	8.788	6	359.065	9.8143	38.916

TABLE 8. Continued

N [a]	$\dfrac{<T>}{K}$	$\dfrac{\Delta T}{K}$	$\dfrac{C_{sat,m}}{R}$ [b]	N [a]	$\dfrac{<T>}{K}$	$\dfrac{\Delta T}{K}$	$\dfrac{C_{sat,m}}{R}$ [b]
9	94.362	9.1318	9.557	3	364.193	9.9215	39.681
9	103.747	9.6051	10.389	4	367.303	13.3870	40.125
8	109.618	10.0152	10.928	6	368.984	10.0385	40.383
9	113.433	9.7457	11.271	3	371.681	4.9860	40.835
8	119.539	9.8052	11.824				
			cr(l)				
1	381.302	6.0669	39.980	1	394.713	6.1892	41.619
4	386.327	8.3788	40.544	1	401.054	6.2085	42.904
1	387.964	7.1520	40.766	13	401.291	5.9460	42.934
2	392.191	15.5357	41.326				
			liquid				
14	412.748	5.7703	46.697	1	422.190	8.1107	47.529
1	414.057	8.1803	46.832	13	428.239	12.0938	48.020
12	415.833	9.7884	46.979	14	431.680	12.0511	48.313
13	416.203	11.9942	46.992	13	439.253	9.9661	48.951
14	420.649	9.9485	47.372	14	441.288	7.1063	49.122

[a] Adiabatic series number.

[b] Average heat capacity for a temperature increment of ΔT with a mean temperature $<T>$.

TABLE 9.   Experimental $c_{x,m}^{II}/R$ values $(R = 8.31451 \text{ J·K}^{-1}\text{·mol}^{-1})$

mass/g	0.016605	0.009995	0.020905	0.014624	0.025187	0.008866
Vol. cell/cm^3 [a]	0.05288	0.05292	0.05288	0.05292	0.05288	0.05288
T/K	$c_{x,m}^{II}/R$	$c_{x,m}^{II}/R$	$c_{x,m}^{II}/R$	$c_{x,m}^{II}/R$	$c_{x,m}^{II}/R$	$c_{x,m}^{II}/R$
	4,5,9,10-Tetrahydropyrene			1,2,3,6,7,8-Hexahydropyrene		
435.0	47.9	47.9	47.6	48.6	48.6	48.6
455.0	49.8	49.6	49.2	50.3	50.2	50.3
475.0	51.3	51.4	50.7	51.8	51.8	52.0
495.0	52.7	52.8	52.2	53.4	53.0	53.9
515.0	53.3	54.3	53.3	54.7	54.7	55.4
535.0	55.1	55.9	55.2	56.3	56.1	57.0
555.0	56.4	57.7	56.4	57.9	57.5	58.5
575.0	57.9	58.7	57.6	59.3	59.1	60.4
595.0	59.5	60.4	59.2	60.9	60.3	62.3
615.0	60.5	62.0	60.8	62.4	61.8	63.1
635.0	61.2	63.3	61.8	63.6	63.4	64.7
655.0	63.0	66.4	63.0	65.2	64.3	66.3
675.0	64.0	68.3	63.8		65.7	
695.0	66.2	70.1	65.3	68.1	67.1	70.3
715.0		69.4 [b]	64.5 [b]	69.9	68.1	72.3
735.0		68.2 [b]	62.7 [b]	71.8	69.7	74.6

a   Volume measured at 298.15 K.
b   These values were not used in the fitting procedures. The lower heat capacities are indicative of sample decomposition.

TABLE 10. Parameters for equations (12) and (14), estimated critical constants and acentric factors. [a]

	4,5,9,10-Tetrahydropyrene		
A	-9.27266	b_0	-0.58943
B	4.11136	b_1	-0.89964
C	-5.24048	b_2	0.89772
D	-2.71688	b_3	-0.73166

$T_c = 900$ K $p_c = 3000$ kPa $\rho_c = 324.3$ kg·m^{-3} $\omega = 0.471$

	1,2,3,6,7,8-Hexahydropyrene		
A	-10.69799	b_0	-0.68250
B	6.77346	b_1	-0.27790
C	-6.85542	b_2	-0.64931
D	-1.61309	b_3	0.55094

$T_c = 920$K $p_c = 3610$ kPa $\rho_c = 313.7$ kg·m^{-3} $\omega = 0.513$

[a] Values for the critical constants and acentric factor are estimates derived from the fitting procedures. See text.

TABLE 11. Values of $C_{v,m}^{II}(\rho = \rho_{sat})/R$ and $C_{sat,m}/R$ ($R = 8.31451$ $J \cdot K^{-1} \cdot mol^{-1}$)

T/K	$C_{v,m}^{II}(\rho = \rho_{sat})/R$	$C_{sat,m}/R$	T/K	$C_{v,m}^{II}(\rho = \rho_{sat})/R$	$C_{sat,m}/R$
		4,5,9,10-Tetrahydropyrene			
420.0	46.7	46.7	580.0	58.0	58.1
440.0	48.3	48.3	600.0	59.3	59.3
460.0	49.8	49.8	620.0	60.4	60.4
480.0	51.3	51.3	640.0	61.5	61.6
500.0	52.7	52.7	660.0	62.6	62.6
520.0	54.1	54.1	680.0	63.6	63.6
540.0	55.5	55.5	700.0	64.5	64.6
560.0	56.8	56.8			
		1,2,3,6,7,8-Hexahydropyrene			
420.0	47.3	47.3	580.0	59.2	59.2
440.0	49.0	49.0	600.0	60.5	60.5
460.0	50.6	50.6	620.0	61.8	61.8
480.0	52.2	52.2	640.0	63.0	63.0
500.0	53.7	53.7	660.0	64.2	64.2
520.0	55.2	55.2	680.0	65.3	65.4
540.0	56.6	56.6	700.0	66.5	66.6
560.0	57.9	57.9			

TABLE 12. Enthalpies of vaporization obtained from the Wagner and Clapeyron equations

T/K	$\Delta_l^g H_m/RK$	T/K	$\Delta_l^g H_m/RK$	T/K	$\Delta_l^g H_m/RK$
4,5,9,10-Tetrahydropyrene					
380.00 [a]	9054±38	500.00	8020±27	620.00	6975±36
400.00 [a]	8875±36	520.00	7853±26	640.00	6782±43
420.00 [a]	8698±34	540.00	7685±26	660.00 [a]	6581±51
440.00	8525±32	560.00	7515±26	680.00 [a]	6371±61
460.00	8355±30	580.00	7340±28	700.00 [a]	6151±72
480.00	8187±28	600.00	7161±31		
1,2,3,6,7,8-Hexahydropyrene					
380.00 [a]	9142±38	500.00	8191±27	620.00	7230±32
400.00 [a]	8980±36	520.00	8035±26	640.00 [a]	7060±37
420.00	8820±34	540.00	7878±26	660.00 [a]	6884±43
440.00	8661±32	560.00	7720±26	680.00 [a]	6704±51
460.00	8503±30	580.00	7560±26	700.00 [a]	6518±61
480.00	8347±29	600.00	7397±28		

[a] Values at this temperature were calculated with extrapolated vapor pressures determined from the fitted Wagner coefficients.

TABLE 13. Molar thermodynamic functions at vapor-saturation pressure [a]

$$(R = 8.31451 \text{ J·K}^{-1}\text{·mol}^{-1})$$

$\dfrac{T}{K}$	$\dfrac{C_{sat,m}}{R}$	$\dfrac{\Delta_0^T S_m}{R}$	$\dfrac{\Delta_0^T H_m}{RT}$	$\dfrac{T}{K}$	$\dfrac{C_{sat,m}}{R}$	$\dfrac{\Delta_0^T S_m}{R}$	$\dfrac{\Delta_0^T H_m}{RT}$
			4,5,9,10-Tetrahydropyrene				
			cr(III)				
5.00	0.064	0.021	0.016	140.00	13.282	13.248	6.954
10.00	0.497	0.170	0.127	160.00	15.122	15.141	7.860
20.00	1.988	0.968	0.683	180.00	17.033	17.032	8.772
30.00	3.324	2.035	1.347	200.00	19.020	18.928	9.697
40.00	4.464	3.151	1.988	220.00	21.078	20.837	10.637
50.00	5.467	4.257	2.585	240.00	23.221	22.762	11.596
60.00	6.400	5.338	3.144	260.00	25.451	24.709	12.576
70.00	7.267	6.390	3.672	280.00	27.746	26.678	13.577
80.00	8.108	7.415	4.174	300.00	30.125	28.673	14.600
90.00	8.948	8.419	4.658	310.00	31.358	29.681	15.121
100.00	9.793	9.405	5.129	319.90 [b]	32.563	30.686	15.642
120.00	11.508	11.342	6.049				
			cr(II)				
290.00 [b]	29.980	28.956	15.507	350.00	37.078	35.236	18.592
298.15	30.924	29.800	15.915	360.00	38.208	36.296	19.122
310.00	32.314	31.032	16.515	370.00	39.272	37.358	19.652
319.90	33.484	32.066	17.023	375.00	39.770	37.888	19.917
320.00	33.495	32.077	17.028	380.00	40.222	38.418	20.181
330.00	34.673	33.125	17.544	385.00 [b]	40.652	38.947	20.444
340.00	35.885	34.178	18.066	385.10 [b]	40.661	38.957	20.449
			cr(I)				
385.10 [b]	39.581	39.039	20.531	405.00	41.417	41.079	21.512
390.00	40.022	39.542	20.773	410.00 [b]	41.894	41.590	21.757
395.00	40.482	40.055	21.020	412.725 [b]	42.155	41.868	21.891
400.00	40.951	40.567	21.266				

TABLE 13. continued

$\dfrac{T}{K}$	$\dfrac{C_{sat,m}}{R}$	$\dfrac{\Delta_0^T S_m}{R}$	$\dfrac{\Delta_0^T H_m}{RT}$	$\dfrac{T}{K}$	$\dfrac{C_{sat,m}}{R}$	$\dfrac{\Delta_0^T S_m}{R}$	$\dfrac{\Delta_0^T H_m}{RT}$
			liquid				
380.00 [b]	43.460	43.149	25.327	520.00	54.133	58.422	31.694
390.00 [b]	44.292	44.289	25.803	540.0	55.49	60.49	32.55
400.00 [b]	45.114	45.420	26.276	560.0	56.79	62.53	33.39
410.00 [b]	45.926	46.544	26.745	580.0	58.06	64.55	34.22
412.725 [b]	46.146	46.849	26.872	600.0	59.27	66.54	35.04
420.00	46.723	47.661	27.211	620.0	60.44	68.50	35.84
440.00	48.297	49.871	28.134	640.0	61.56	70.44	36.62
460.00	49.817	52.051	29.044	660.0	62.63	72.35	37.40
480.00	51.292	54.203	29.940	680.0	63.65	74.23	38.15
500.00	52.745	56.326	30.824	700.0	64.62	76.09	38.89

1,2,3,6,7,8-Hexahydropyrene

cr(II)

$\dfrac{T}{K}$	$\dfrac{C_{sat,m}}{R}$	$\dfrac{\Delta_0^T S_m}{R}$	$\dfrac{\Delta_0^T H_m}{RT}$	$\dfrac{T}{K}$	$\dfrac{C_{sat,m}}{R}$	$\dfrac{\Delta_0^T S_m}{R}$	$\dfrac{\Delta_0^T H_m}{RT}$
5.00	0.031	0.010	0.008	180.00	17.544	16.647	8.908
10.00	0.255	0.084	0.063	200.00	19.560	18.599	9.872
20.00	1.481	0.597	0.437	220.00	21.650	20.560	10.847
30.00	2.927	1.474	1.029	240.00	23.838	22.537	11.838
40.00	4.234	2.500	1.671	260.00	26.120	24.535	12.848
50.00	5.375	3.569	2.299	280.00	28.488	26.556	13.880
60.00	6.419	4.643	2.900	298.15	30.734	28.415	14.837
70.00	7.362	5.704	3.471	300.00	30.966	28.606	14.936
80.00	8.279	6.747	4.015	320.00	33.535	30.686	16.018
90.00	9.168	7.774	4.538	340.00	36.216	32.799	17.126
100.00	10.056	8.786	5.045	360.00	39.051	34.948	18.265
120.00	11.866	10.779	6.031	370.00	40.557	36.039	18.847
140.00	13.704	12.745	6.995	377.00 [b]	41.607	36.809	19.260
160.00	15.600	14.698	7.951				

TABLE 13. continued

$\dfrac{T}{K}$	$\dfrac{C_{sat,m}}{R}$	$\dfrac{\Delta_0^T S_m}{R}$	$\dfrac{\Delta_0^T H_m}{RT}$	$\dfrac{T}{K}$	$\dfrac{C_{sat,m}}{R}$	$\dfrac{\Delta_0^T S_m}{R}$	$\dfrac{\Delta_0^T H_m}{RT}$
			cr(l)				
377.00 [b]	39.446	39.992	22.443	395.00	41.505	41.880	23.265
380.00	39.790	40.306	22.579	400.00	42.074	42.405	23.497
385.00	40.363	40.830	22.806	405.00 [b]	42.641	42.931	23.730
390.00	40.935	41.355	23.035	407.635 [b]	42.939	43.209	23.853
			liquid				
380.00 [b]	43.860	45.384	28.036	540.0	56.57	62.99	34.69
390.00 [b]	44.739	46.535	28.453	560.0	57.93	65.08	35.49
400.00 [b]	45.610	47.679	28.871	580.0	59.25	67.13	36.29
407.635 [b]	46.270	48.547	29.191	600.0	60.53	69.16	37.08
420.00	47.328	49.946	29.709	620.0	61.79	71.17	37.86
440.00	49.015	52.186	30.549	640.0	63.02	73.15	38.62
460.0	50.63	54.40	31.39	660.0	64.22	75.11	39.38
480.0	52.20	56.59	32.22	680.0	65.43	77.04	40.13
500.0	53.70	58.75	33.05	700.0	66.63	78.96	40.87
520.0	55.16	60.89	33.87				

[a] Values listed in this table are reported with one digit more than is justified by the experimental uncertainty. This is to avoid round-off errors in the calculation of values listed in table 14.

[b] Values at this temperature were calculated with graphically extrapolated heat capacities.

TABLE 14. Thermodynamic properties in the ideal-gas state
(R = 8.31451 $J \cdot K^{-1} \cdot mol^{-1}$ and p° = 101.325 kPa)

$\dfrac{T}{K}$	$\dfrac{\Delta_0^T H_m^\circ}{RT}$	$\dfrac{\Delta_{imp}H_m^\circ}{RT}$ [a]	$\dfrac{\Delta_0^T S_m^\circ}{R}$	$\dfrac{\Delta_{imp}S_m^\circ}{R}$ [b]	$\dfrac{\Delta_f H_m^\circ}{RT}$	$\dfrac{\Delta_f S_m^\circ}{R}$	$\dfrac{\Delta_f G_m^\circ}{RT}$
			4,5,9,10-Tetrahydropyrene				
380.00 [c,d]	49.15±0.10	0.00	58.39±0.11	0.00	36.39±0.25	−73.10±0.11	109.49±0.24
400.00 [c,d]	48.46±0.09	0.00	60.20±0.10	0.00	34.01±0.24	−73.68±0.10	107.69±0.22
420.00 [c]	47.92±0.09	0.00	62.01±0.09	0.00	31.87±0.22	−74.21±0.09	106.08±0.22
440.00	47.51±0.08	0.00	63.82±0.09	0.00	29.96±0.21	−74.68±0.09	104.64±0.21
460.00	47.22±0.07	0.01	65.63±0.08	0.01	28.24±0.20	−75.11±0.08	103.35±0.20
480.00	47.01±0.07	0.01	67.43±0.08	0.01	26.68±0.19	−75.50±0.08	102.18±0.19
500.00	46.89±0.06	0.02	69.22±0.08	0.02	25.27±0.19	−75.84±0.08	101.11±0.19
520.00	46.83±0.06	0.03	71.00±0.08	0.03	23.99±0.18	−76.16±0.08	100.15±0.18
540.00	46.83±0.06	0.05	72.77±0.08	0.04	22.81±0.17	−76.45±0.08	99.26±0.18
560.00	46.88±0.07	0.07	74.52±0.09	0.05	21.73±0.17	−76.71±0.09	98.44±0.18
580.00	46.97±0.09	0.09	76.26±0.10	0.07	20.73±0.17	−76.95±0.10	97.69±0.18
600.00	47.10±0.10	0.13	77.98±0.12	0.09	19.81±0.18	−77.18±0.12	96.99±0.19
620.00	47.25±0.12	0.16	79.68±0.14	0.12	18.94±0.18	−77.39±0.14	96.33±0.21
640.00	47.43±0.14	0.21	81.37±0.16	0.16	18.14±0.20	−77.59±0.16	95.73±0.22
660.00 [c]	47.63±0.16	0.26	83.04±0.18	0.20	17.38±0.21	−77.77±0.18	95.15±0.24
680.00 [c]	47.85±0.18	0.33	84.68±0.20	0.24	16.67±0.22	−77.95±0.20	94.62±0.26
700.00 [c]	48.08±0.20	0.40	86.31±0.23	0.30	15.99±0.24	−78.12±0.23	94.11±0.27

TABLE 14. continued

$\dfrac{T}{K}$	$\dfrac{\Delta_0^T H_m^\circ}{RT}$	$\dfrac{\Delta_{imp}H_m^\circ}{RT}$ [a]	$\dfrac{\Delta_0^T S_m^\circ}{R}$	$\dfrac{\Delta_{imp}S_m^\circ}{R}$ [b]	$\dfrac{\Delta_f H_m^\circ}{RT}$	$\dfrac{\Delta_f S_m^\circ}{R}$	$\dfrac{\Delta_f G_m^\circ}{RT}$
			1,2,3,6,7,8-Hexahydropyrene				
380.00 [c,d]	52.09±0.10	0.00	60.53±0.11	0.00	16.40±0.32	−87.50±0.11	103.91±0.31
400.00 [c,d]	51.32±0.09	0.00	62.41±0.10	0.00	14.90±0.30	−88.20±0.10	103.10±0.29
420.00	50.71±0.09	0.00	64.29±0.09	0.00	13.58±0.29	−88.83±0.09	102.41±0.28
440.00	50.24±0.08	0.00	66.16±0.09	0.00	12.40±0.27	−89.41±0.09	101.80±0.27
460.00	49.88±0.07	0.01	68.03±0.09	0.01	11.35±0.26	−89.93±0.09	101.27±0.26
480.00	49.62±0.08	0.01	69.89±0.09	0.01	10.41±0.25	−90.40±0.09	100.81±0.25
500.00	49.45±0.09	0.02	71.74±0.10	0.01	9.57±0.25	−90.83±0.10	100.40±0.25
520.00	49.35±0.10	0.03	73.58±0.11	0.02	8.81±0.24	−91.23±0.11	100.04±0.26
540.00	49.32±0.11	0.04	75.41±0.13	0.03	8.12±0.24	−91.59±0.13	99.71±0.26
560.00	49.33±0.13	0.05	77.22±0.15	0.04	7.50±0.24	−91.92±0.15	99.42±0.27
580.00	49.40±0.14	0.07	79.02±0.17	0.06	6.94±0.24	−92.22±0.17	99.16±0.29
600.00	49.51±0.16	0.10	80.80±0.19	0.07	6.43±0.25	−92.50±0.19	98.92±0.30
620.00	49.65±0.17	0.13	82.57±0.21	0.10	5.95±0.25	−92.75±0.21	98.71±0.32
640.00 [c]	49.82±0.19	0.17	84.32±0.23	0.12	5.52±0.26	−92.99±0.23	98.51±0.33
660.00 [c]	50.02±0.21	0.21	86.06±0.25	0.16	5.13±0.27	−93.20±0.25	98.33±0.35
680.00 [c]	50.25±0.23	0.26	87.79±0.27	0.20	4.76±0.28	−93.39±0.27	98.16±0.37
700.00 [c]	50.50±0.25	0.32	89.51±0.29	0.24	4.43±0.30	−93.57±0.29	98.00±0.39

[a] Gas-imperfection correction included in the ideal-gas enthalpy.

[b] Gas-imperfection correction included in the ideal-gas entropy.

[c] Values at this temperature were calculated with extrapolated vapor pressures calculated from the fitted Wagner equation parameters.

[d] Values at this temperature were calculated with extrapolated liquid-phase heat capacities.

TABLE 15. Comparison of experimental and calculated sublimation pressures

$\frac{T}{K}$	$\frac{p\{cr(l)\}}{Pa}$ [a]	$\frac{p(liquid)}{Pa}$ [b]	$\frac{p(calc)}{Pa}$ [c]	$\frac{\Delta(p)}{Pa}$ [d]
4,5,9,10-Tetrahydropyrene				
385.000 [e]	18.3	25.7	18.1	0.2
390.000	26.2	34.7	26.1	0.1
395.002	37.3	46.4	37.2	0.1
405.003	74.0	80.7	73.4	0.6
410.002	102.2	105.3	101.8	0.4
1,2,3,6,7,8-Hexahydropyrene				
390.004	20.1	25.3	20.0	0.1
395.001	28.7	34.0	28.7	0.0
400.001	40.9	45.2	40.9	0.0
405.003	57.6	59.6	57.6	0.0

[a] Sublimation pressure measured in inclined piston.

[b] Vapor pressure for supercooled liquid calculated using the Wagner equation parameters listed in table 5.

[c] Sublimation pressure calculated using equations (21) or (22).

[d] $p\{cr(l)\}$ − $p(calc)$ is the difference between measured and calculated values of the sublimation pressure.

[e] This temperature is below the cr(l)-to-cr(ll) transition temperature. The difference between the cr(l) and cr(ll) sublimation pressures is not significant this close to T_{trs} (385.1 K).

END

DATE
FILMED
2/2/93